Article type: **Review**

Fiber Crossbars: An Emerging Architecture of Smart Electronic Textiles

Xuhui Zhou, Zhe Wang, Ting Xiong, Bing He, Zhixun Wang, Haozhe Zhang, Dongmei Hu, Yanting Liu, Chunlei Yang, Qingwen Li, Ming Chen, Qichong Zhang*, and Lei Wei**

X.H. Zhou, Dr. Z. Wang, Dr. T. Xiong, Dr. B. He, Dr. Z.X. Wang, H.Z. Zhang, Dr. Y.T. Liu, Prof. L. Wei

School of Electrical and Electronic Engineering, Nanyang Technological University, 50 Nanyang Avenue, 639798, Singapore

Dr. D.M. Hu, Prof. Q.W. Li, Prof. Q.C. Zhang

Key Laboratory of Multifunctional Nanomaterials and Smart Systems, Suzhou Institute of Nano-Tech and Nano-Bionics, Chinese Academy of Sciences, Suzhou 215123, China

Prof. C.L. Yang, Prof. M. Chen

Shenzhen Institute of Advanced Technology, Chinese Academy of Sciences, Shenzhen 518055, China

Prof. L. Wei

The Institute for Digital Molecular Analytics and Science (IDMxS), Nanyang Technological University, 59 Nanyang Drive, 636921, Singapore

[*] E-mail: ming.chen2@siat.ac.cn; qczhang2016@sinano.ac.cn; wei.lei@ntu.edu.sg

ABSTRACT: Smart wearables have had a significant impact on people's daily lives, enabling personalized motion monitoring, realizing the Internet of Things (IoTs), and even reshaping the next generation of telemedicine systems. Fiber crossbars (FCs), constructed by crossing two fibers, have become an emerging architecture among the accessible structures of state-of-the-art smart electronic textiles. The mechanical, chemical, and electrical interactions between crossing fibers result in extensive functionalities, leading to the significant development of innovative electronic textiles employing FCs as their basic units. This review provides a timely and comprehensive overview of the structure designs, material selections, and assembly techniques of FC-based devices. The recent advances in FC-based devices are summarized, including multipurpose sensing, multiple-mode computing, high-resolution display, high-efficient power supply, and large-scale textile systems. Finally, current challenges, potential solutions, and future perspectives for FC-based systems are discussed for their further development in scale-up production and commercial applications.

Keywords: Fiber crossbars; functional fibers; smart textiles; wearable devices integrated systems

1. Introduction

Smart wearables play an essential and active role in our daily lives, particularly in consumer electronics, remote medical healthcare, exercise and sports monitoring, and the Internet of Things (IoTs).[1-3] The dominant products of smart wearables, including smartwatches, bands, glasses, and wearable augmented or virtual reality (AR/VR) devices, are currently based on either rigid semiconductor components or flexible thin films. These devices are commonly embedded in clothing, attached to the skin, or worn as accessories. However, combining functional devices and wearable substrates can compromise the breathability, long-term wearing comfort, and deformation capacity of these smart wearables.[4-6]

Smart textiles made of functional fibers are promising alternatives to traditional wearable devices because of their appealing properties, such as better breathability, comfort, and deformability, as well as high strength, dynamic bending elasticity, and lightweight characteristics.[7] Essential breakthroughs in structural designs, accessible materials, device geometries, morphologies, and biomechanics have enabled smart textiles to have unique applications.[8] Fiber crossbars (FCs), a type of textile architecture, have become a favorable basic unit for state-of-the-art smart wearables. A crossbar consists of two interlaced fibers, and electronic devices are constructed at the cross points between fibers, as shown in **Figure 1**. Certain stimuli, such as mechanical force, chemical reaction, and electrical and light signals, can be transmitted between fibers and induce corresponding responses of the FC, including resistance change[9], capacitance change[10], conductance change[11], and lighting[12]. These essential stimuli-response processes are powered by an FC energy source. Therefore, in FC-based smart textiles, fibers are not isolated but have frequent interactions with each other, forming functional devices at the cross points between fibers. Multiple FCs can be combined into various textile structures, such as plain weave and knit, to create a large array with more sophisticated functions.

However, fabricating FC-based electronics that integrate multiple materials and complex

multilayer structures can be challenging. Planar device fabrication techniques, such as photolithography, cannot be directly adapted to fibers with highly curved surfaces. Therefore, various fiber-compatible fabrication methods, including fiber spinning, coating, confinement wrapping, thermal drawing, and in-situ growth, have been developed to form FC-based devices. Conducting, semiconducting, and insulating materials are widely used in FC-based devices.[13] Conducting materials such as pure metals (e.g., Cu[14], Ag[15]) and carbon-based materials (e.g., carbon nanotubes (CNTs)[16], graphene[17]); semiconducting materials such as inorganic semiconductors (e.g., Si[18]) and organic semiconductors (e.g., poly (3,4-ethylene dioxythiophene) polystyrene sulfonate (PEDOT:PSS)[19], polypyrrole (PPy)[11]); and insulating materials such as metal oxides (e.g., AlO_x[20], TiO_x[21]) and organic insulators (e.g., polydimethylsiloxane (PDMS[10]), polyvinylidene fluoride (PVDF)[22]) have been utilized as functional materials to form FC-based devices. Among them, metallics and inorganic semiconductors have satisfactory and stable electrical properties (e.g., conductivity and relative permittivity), but are too rigid to provide sufficient wearing comfort. In comparison, organic materials are highly flexible, lightweight, and compatible with solution-based processing, but generally have inferior electrical properties and stabilities.[23] Carbon-based materials have excellent conductivities, comparable to metals. However, their complex deposition and synthesis methods make them costly for FC-based devices.[24] Previous studies have also reported other functional materials for FC-based devices, including inorganic compounds[25] and biomaterials[26].

This review provides a comprehensive overview of the recent advances in FCs that enable the integration of smart wearable electronics into daily life. First, we systematically summarize the design principles, working mechanisms, materials, structures, and fabrication strategies of FC-based devices. Next, we present the latest applications of FC-based devices in wearable electronics, including sensing, computing, display, and power supply. We also highlight the current challenges and potential trends in developing FC-based wearable products based on the

current developments. Finally, we offer perspectives on the future of FC-based wearable textile systems that are highly integrated and intelligent.

2. Design principles of FC-based devices

An FC unit consists of two interlaced fibers where functional devices are constructed at the cross points. Multiple FC units can form a large array, working collaboratively as a complex functional module[27]. **Figure 2** depicts the design principles and considerations of FC-based devices, including FC-based resistors, capacitors, piezoelectric nanogenerators (PENGs), triboelectric nanogenerators (TENGs), memristors, organic electrochemical transistors (OECTs), field-effect transistors (FETs), light-emitting diodes (LEDs), luminescence, and solar cells.

2.1 FC-based resistors

There are two main types of FC-based resistors: contact resistance[28] and internal resistance[29]. Contact resistors consist of two interlaced warp and weft fibers, forming a sandwich structure with two resistive layers and a small middle gap, as shown in **Figure 2a**.[9] When an external force is applied at the cross point, stretching along the fibers increases the contact area and strength, reducing the contact resistance (R_c) significantly. Pure metals and their nanostructures (e.g., Cu[16]) are commonly used as the resistive layer due to their high conductivity. Conducting polymers (e.g., PEDOT[9]) and carbon-based materials (e.g., CNT[30], carbon black[31]) are also used for their flexibility, although they have lower conductivity.

Figure 2a also illustrates an FC-based internal resistor that contains a conductive channel within the fiber, in contrast to the contact resistor.[32] When pressure is applied to the warp fiber, this can lead to geometrical deformations or the formation of cracks in the resistive layers of the weft fiber, resulting in changes in the internal resistance (R_i).[33] Cracks are often formed due to the mechanical mismatch between different parts of the fiber. Carbon-based materials such as CNTs, graphene, GO, and carbides are often used as the internal resistive layer because they can produce dense cracks to achieve a large resistance change when an external force is

applied.[34-37] For instance, when graphene-coated fibers are subjected to a tensile strain, the decrease in the overlapped area between the graphite sheets induced by crack formation leads to a significant increase in R_i, which is restored when the strain is released.[38] This phenomenon has also been observed in other elastic fibers and yarns coated with carbon-based materials.[28]

2.2 FC-based capacitors

Figure 2b shows an FC-based plate capacitor constructed by interlacing two warp and weft fibers. Each fiber has a conductive core that acts as an electrode and is coated with an insulating dielectric material, forming a capacitor with two electrodes and a middle insulator. When voltage is applied, opposite charges accumulate on the electrodes, forming a mutual capacitance (C_M). The value of C_M depends on the electrode area (A), spacing (d), and the dielectric constant (ε_r) of the insulator, which changes when pressure is applied at the cross point[39]. To achieve high sensitivity, various insulating polymers, such as polyurethane[40] and Eco-flex rubber[41], have been used for the insulator due to their flexibility and high dielectric constants. The elastic insulating polymers undergo significant deformations of A and d under pressure, which substantially changes the C_M. Common electrode materials include metals, such as Ag[10], and conductive polymers, such as PEDOT:PSS[42]. In addition to the classical plate capacitor, aqueous and gel electrolyte FC-based supercapacitors have also been developed.

2.3 FC-based PENGs

Piezoelectric nanogenerators (PENGs) are devices that convert mechanical energy into electrical energy using the piezoelectric effect.[43] An FC-based PENG consists of two interlaced warp and weft fibers, forming a sandwich structure composed of two electrodes and the middle piezoelectric dielectric layer. The function of the warp fiber is to transmit pressure to the weft fiber, as shown in **Figure 2c**.[44] When a load is applied, the atomic structure of the piezoelectric layer changes, forming a moment-changing electric dipole, which induces a piezoelectric potential between the inner and outer electrodes of the weft fiber.[45] Piezoelectric ceramics, such as lead zirconate titanate (PZT)[46] and barium titanate[47], have high mechanical

strength, power density, and chemical inertness to resist moisture, but their inherent rigidity limits their use in FCs and other wearables.[48] Piezoelectric polymers, such as polyvinylidene fluoride (PVDF)[49] and its copolymer PVDF-TrFE[50], have lower piezoelectric coefficients and electromechanical coupling coefficients than piezoelectric ceramics but are still the preferred choice because of their excellent flexibility and softness.[51]

2.4 FC-based TENGs

TENGs are devices that convert mechanical energy into electrical energy by utilizing the triboelectric effect and electrostatic induction.[52] An FC-based TENG is constructed by placing two electrodes in two interlaced warp and weft fibers (**Figure 2d**), in a single fiber (**Figure 2e**), or between one fiber and ground (**Figure 2f**). The working mechanism of FC-based TENGs is described by the contact-separate model and single-electrode model.[53] When two triboelectric dielectric layers get in contact under an external force, electrification occurs, generating opposite polarized charges with the same amount on the interfaces. Positive and negative charges are correspondingly induced in the two electrodes due to the electrostatic induction effect. When the gap between the two triboelectric layers widens, i.e., one fiber moves away from the other, the changing electrical potential difference drives charges to flow in the closed circuit. For TENG devices, the triboelectric series is an important reference for selecting triboelectric materials. The further two materials are from each other on the triboelectric series, the easier charge is transferred during each contact-and-separation cycle.[45] The currently widely used triboelectric materials for FC-based TENGs include polymers such as PVDF[22], PDMS[54], SEBS[55], and silicone rubbers[56].

2.5 FC-based memristors

A memristor is a device that can change its resistance state between high and low resistance states using direct current or programmable pulse voltages. It is a non-linear resistance-switching device that is related to magnetic flux and electric charge. An FC-based memristor is made up of two interlaced warp and weft fibers with a pair of electrodes, namely a top and a

bottom electrode, separated by a middle memristive layer, as shown in **Figure 2g**.[57] There are two categories of recent FC-based memristors: interfacial type and filamentary type.[58] For the interfacial type, both electrodes are electrochemically inert, and resistance switching occurs through Schottky Emission and Fowler-Nordheim Tunneling.[59] The memristive layer is generally made of n-type oxides such as TiO_2[59] and barium strontium titanate (BST)[60], which acts as a donor. During switching, the density of oxygen vacancies inside the memristive layer affects the resistance state of the memristor. For filamentary-type memristors, there are two basic switching mechanisms: electrochemical-metallization and thermal-chemical.[61] Electrochemical-metallization switching relies on conductive filament formations due to ion migration[62], while thermal-chemical switching relies on conductive filament formations due to thermal-chemical reactions such as Joule heating.[58] Memristive layers made of pure metals (e.g., Ni[63]), metal oxides (e.g., Al_2O_3[20]), long chain-shaped organics (e.g., electrophoretic-deposited deoxyribonucleic acid (DNA)[26]), and carbon-based materials (e.g., reduced GO[64]) are widely used in CFC-based memristors to acquire high ON/OFF ratio and stability.

2.6 FC-based transistors

A transistor is an electronic device that amplifies or switches electrical signals and power.[65] There are two main types of FC-based transistors, namely OECTs and FETs. An FC-based OECT is made up of interlaced warp gate fiber and weft source-drain fiber, as shown in **Figure 2h**. The gate fiber is a conducting wire, while the source-drain fiber is an ordinary fiber/yarn coated with electrical conducting polymers, which establish a channel for charges to flow through. By applying a gate voltage (V_g), the drain-source current (I_{ds}) can be precisely modulated through doping and de-doping processes. During this process, ions are injected or removed from the electrical conducting polymer, resulting in reversible ion exchange to achieve multilevel conductance modulations. Doped PPy nanowires[67] and PEDOT:PSS[68] have been widely used as electrical conducting polymer channels in FC-based OECTs due to their high conductivity, flexibility, and stability in the air.

An FC-based FET is made up of two interlaced fibers: the warped source and drain fibers and the weft gate fiber, as depicted in **Figure 2i**. The "bottom-gate top-contact" architecture is a typical design of an FC-based FET where the channel semiconductor layers and gate insulators are deposited on the gate fiber, and the other two conducting wires are connected to the pads on the gate fiber as the source and drain port, respectively.[69] A specific gate voltage induces field-effect doping, which occurs in the thin interfacial region near the channel or insulating layer of the FETs, thus switching it between the ON and OFF states.[65] FC-based FETs are categorized into two types: inorganic FETs that use inorganics as the channel material and organic FETs (OFETs) that use organics as the channel material. For inorganic FETs, metal oxides such as IGZO[67] and carbon-based materials like CNT[70] have been widely used as the channel material due to their high electron mobility, high ON/OFF ratio, and low leakage current. In contrast, for OFETs, π-conjugated semiconductor polymers such as pentacene[71] and P3HT[72] are commonly used as the channel layer due to their flexibility and skin affinity, despite their lower electric performance, thermal stability, and deposition surface topography compared to inorganic metal oxides.[73]

2.7 FC-based lighting devices

Wearable lighting electronics are becoming increasingly popular due to their ability to display information and interact with the wearer.[74] An FC-based lighting device is made up of two interlaced fibers: the weft lighting fiber serves as the light source, and the warp connect fiber acts as an electrode for the device, as illustrated in **Figures 2j-k**. The primary lighting materials are deposited layer by layer onto the lighting fiber, and the device consists of either LEDs or luminescent elements as the primary sources of light.

An FC-based LED has a structure like that of commercial thin-film LEDs, consisting of a pair of cathode and anode electrodes and middle light emitting layers, as shown in **Figure 2j**. Under a DC forward bias, photons are released when electrons from the cathode and holes from the anode recombine in a quantum well active region or a double heterostructure passing

through a doped semiconductor p-n junction.[75] The light-emitting layer of FC-based LEDs typically consists of organic materials (e.g., Ir(ppy)2(acac)[75] and phosphorescent[76]), which are highly compatible with existing low-cost solution processing techniques.

An FC-based electroluminescence device is composed of a pair of bottom and top electrodes with luminescent phosphor particles blended with insulating materials in between, as shown in **Figure 2k**. When an alternating voltage is applied to the medium around the transition metal doped ZnS, the phosphor particles emit light. The device continuously releases visible photons by repeatedly relaxing the luminescent center of the phosphor with the application of an alternating current (AC) electric field through the connected fibers.[77] Typically, Cu-doped ZnS is used as the luminescent phosphor in FC-based electroluminescence devices.[12] On the other hand, an FC-based mechanoluminescence device is composed of a weft mechanoluminescent fiber as the light source and a warp fiber that transmits the pressure to the mechanoluminescent fiber to excite luminescence, as shown in **Figure 2k**. The light-emitting phenomenon in mechanoluminescence occurs when the carriers in shallow traps are de-trapped under mechanical stress. Two mechanisms, stress-induced and triboelectricity-induced, have been proposed to explain the mechanoluminescent effects.[78] Cu-doped ZnS phosphor is also the commonly used luminescent source of FC-based mechanoluminescence devices.[79]

2.8 FC-based solar cells

An FC-based solar cell consists of two interlaced fibers: the weft battery fiber as the energy supplier and the warp connect fiber as an electrode of the solar cell, as shown in **Figure 2l**. The main photovoltaic materials are deposited layer by layer on the battery fiber. To operate, the solar cell requires three main steps: (1) absorption of sunlight, generating excitons (bound electron-hole pairs) and unbound electron-hole pairs via excitons; (2) separation of opposite type charge carriers; and (3) extraction of the carriers to an external circuit to generate a photovoltaic potential U.[80] Metal oxide (e.g., ZnO[81]) and metal iodides (e.g., CuI[82]) are commonly used as electron and hole transport layers, as well as active layers, while in some

cases polymer conductors and semiconductors (e.g., PEDOT:PSS and PTB7:PC71BM[83]) are used as electrodes and charge carrier transporters of the FC-based solar cells, similar to commercial planar solar cells.

3. Fabrication strategies to form FC-based devices

Several fabrication methods have been developed to create electrodes and functional layers on curved fiber surfaces or inside fibers. These methods are summarized in **Figure 3** and can be categorized into five main types: fiber spinning, coating, confinement wrapping, thermal-drawing, and in-situ growth.

3.1 Fiber spinning

Fiber spinning is a widely used technique for forming single-strand FC fibers (wet spinning) or wrapping functional fibers around core wires to create twisted FC devices (electrospinning). This straightforward fiber extrusion method allows for the direct formation of fibers. In wet spinning, a solution is extruded through a spinneret, creating a fiber as the solvent evaporates. In electrospinning, an electric field is used to draw a charged solution or melt from a spinneret, resulting in the formation of fibers.

3.1.1 Wet spinning

Wet spinning is a solution-based technique used to create continuous FC fibers with functional layers directly formed during the process, as shown in **Figure 3a**.[84] The process comprises three essential components: a spin pump featuring a small inner diameter spinneret, a coagulation bath consisting of a mixture of solvent and non-solvent, and a fiber collector. The material to be spun is dissolved in a solvent and extruded through the spinneret into the coagulation bath. The solvent and non-solvent in the bath cause the solution to coagulate. Wet spinning is advantageous because it can create complete, single-strand fibers in one step with minimal post-processing. However, the conductivity and mechanical strength of the resulting fiber are often low, making it prone to peeling and breaking during long-term use. Wet spinning has been used to create conductive cores for FC-based capacitors, mainly using polymers (e.g.,

PEDOT:PSS[85]) and carbon-based materials (e.g., GO[86]).

3.1.2 Electrospinning

The electrospinning method is ideal for forming polymer fibers with ultra-large surface areas and deformable porous microstructures, and benefits from low processing temperatures and material versatility, as shown in **Figure 3b**.[87] The basic setup for electrospinning comprises three main parts: a high-voltage power supply, a spinneret, and a rotating conductive core wire. During electrospinning, a Coulomb repulsion is generated by the high DC voltage supply connected to the spinneret tip, which extrudes fibers that wrap around the core wire to form a twisted fiber surface.[87] However, like wet spinning, the resulting electrospun fibers lack sufficient mechanical strength. The electrospinning process is widely used to form fibrous resistive layers of FC-based resistors[16], dielectric layers of FC-based capacitors[40], piezoelectric layers of FC-based PENGs[49], and triboelectric layers of FC-based TENGs[88], with polymers such as PVDF, PVDF-TrFE, and polyurethane commonly used as main materials.

3.2 Coating

Coating processes involve applying a solution onto FC fiber substrates, primarily through dip-coating and evaporation, to create coaxial films on the outer surfaces of fiber cores.[89] The dip-coating process typically involves immersing the fiber core in the coating solution, keeping the fiber core inside the solution, pulling up the fiber core, and then evaporating the solvent to form a thin solid layer, as shown in **Figure 3c**. In some cases, the processed fiber is passed through a thin tube to improve surface quality and thickness control of the coating.[90] While these techniques may result in nonuniform film formation (e.g., the "pearl necklace" phenomenon caused by capillary instability) and low coating adhesion strength, they are widely used for depositing functional layers of FCs in a large scale due to their processing simplicity and continuity characteristics. These methods have been used to achieve resistive layers of FC-based resistors[31], piezoelectric layers of FC-based PENGs[50], triboelectric layers of FC-based TENGs[14], gate insulators and channels of FC-based transistors[91], lighting materials of FC-

based LEDs[76] and luminescence[79], and photovoltaic materials of FC-based solar cells[82]. The materials used for depositing include polymers (e.g., PEDOT:PSS[76] and PVDF-TrFE[50]) and parts of metal compounds (e.g., Cu-doped ZnS phosphor[79]).

3.3 Confinement wrapping

Confinement wrapping uses a scrolling method to wrap certain materials inside a film shell to form FC fibers, which involves three main steps: (1) preparation of soft substrates; (2) deposition of functional materials onto the substrate; and (3) scrolling the "substrate-functional material" double-layer structure to form coaxial fibers, as shown in **Figure 3d**. In general, the confinement wrapping technique has good material suitability, and any material that can be successfully deposited on the soft substrate can be scrolled into functional fibers with suitable sizes. However, confinement wrapping for the ultra-thin film is complicated and challenging to be continuously produced over a large scale. Recently, confinement wrapping has been used to form fiber electrodes of FC energy source, while carbon-based materials (e.g., CNTs) and metal compound/Si are used as the soft substrate material and functional material, respectively.[92]

3.4 Thermal drawing

Thermal drawing is a direct fiber formation technique used to produce kilometer-long and sub-millimeter diameter FC fibers with complex inner structures from a macroscopic preform.[93] The process involves two main stages: (1) preparing thermoplastic material-based preforms, and (2) feeding the preform into the furnace of a drawing tower (at the speed of v_f), and then drawing it (at the speed of v_d) by a capstan at a temperature higher than the glass transition temperature (T_g) of the preform cladding, as shown in **Figure 3e**.[94] The thermal drawing process has been used to form polymers, such as PVDF and PVDF/barium titanate composite, for piezoelectric layers of FC-based PENGs[95] and triboelectric layers of FC-based TENGs[22]. Compared to other FC fiber fabrication strategies, the thermal drawing technique can realize continuous and large-scale fiber formation while producing FC fibers with high mechanical strength, stable electrical properties, and precise internal substructures.

3.5 In-situ growth

In-situ growth refers to the process in which thin films grow continuously in the same place. Unlike the surface coating, adhesives are not required for the entire growth period. In-situ polymerization, electroplating, and hydro/solvothermal processing are typical solution-based techniques used for in-situ growth to form nanoarray films on the surface of FC fibers.

3.5.1 In-situ polymerization

In-situ polymerization is a technique used to prepare polymer nanocomposites from nanoparticles on FC fibers. This technique involves two main steps: (1) spreading nanoparticles in liquid monomers with relatively low molecular weight to generate a homogeneous mixture, and (2) initiating the polymerization reaction by adding appropriate initiators, as shown in **Figure 3f**. The resulting nanocomposites are composed of polymer molecules bound to nanoparticles.[96] In-situ polymerization has two advantages: (1) the process can retain the air permeability, mechanical properties, and flexibility of the fiber after polymerization, and (2) fibers and polymer are mechanically bonded, so the polymer layer is not easy to separate from the fiber substrate during deformation. However, in-situ polymerization has a limited range of material selections due to the synthesis mechanism. It is only suitable for growing metals (e.g., Cu electrodes of FC-based resistors[97]) and polymers (e.g., PPy-doped channels of FC-based OECTs[11]).

3.5.2 Electroplating

Electroplating, also known as electrochemical deposition, is a common non-spontaneous solution-based synthesis technique for forming conductive or semiconductive films on a conducting FC fiber substrate through redox reactions. The three-electrode method is a widely used electroplating technique that involves three distinct electrodes: the working electrode (i.e., fiber), the reference electrode, and the counter electrode, as shown in **Figure 3g**.[98] In this technique, a monomer solution is initially loaded into a cell, and when a DC is applied, the monomers undergo chemical polymerization on the fiber surface. Despite its advantages, such

as low cost and ease of on-electrode synthesis, the morphology and uniformity of the coating depend on the intrinsic properties of the polymerization materials used, which limits its deposition applicability and controllability. Additionally, the adhesion strength of the film is often insufficient, and it may detach during long-term use. Currently, electroplating is being used to form metal nanowires, such as NiO nanowires[99], and carbon memristive layers, such as GO[64], for FC-based memristors.

3.5.3 Hydro/solvothermal processing

Hydro/solvothermal processing is a method for synthesizing materials using high-pressure and high-temperature reactions in a liquid solvent. The process is often used to create materials that are difficult to make through other methods, such as nanoparticles, nanowires, and thin films, as illustrated in **Figure 3h**. It offers several advantages over other methods, including the ability to synthesize nanomaterials that are unstable at high temperatures, generate materials with a minimal loss under high vapor pressures, and precisely control the composition of the synthesized nanomaterials through liquid or multiphase chemical reactions. However, it is important to note that fibers made of non-heat-resistant materials (such as low-melting-point polymers) may not be suitable for prolonged heat treatment. Recently, hydro/solvothermal synthesis has been used to produce electrode materials for FC-based supercapacitors and other energy devices.[100]

3.6 Fiber assembly

FC fibers can be assembled into fabrics and textiles electronics using various methods. Generally, for FC-based resistors, capacitors, and nanogenerators, the two weft and warp fibers do not need to fit tightly but just need to simply contact each other. Industrial textile processes, such as weaving or knitting, can assemble these devices. For example, in weaving, yarns are interlaced at right angles to create a fabric. The lengthwise threads are held under tension on a loom, while the crosswise threads are interwoven using a shuttle. This interlacing creates a strong and stable fabric. In knitting, loops of yarn are interlocked to create a fabric. The yarns

are held by knitting needles or a knitting machine, and the loops are created by pulling the yarns through the existing loops. Knitted fabrics are stretchy and are suitable for creating stretchable smart wearables.[14] For FC-based transistors, light devices, and solar cells, a strong and high-quality electrical connection made by the soldering process is essential for maintaining a stable power supply, electrical conductivity, and signal integrity of the weft and warp fibers being joined. This is especially important in devices that undergo stretching, vibration, and distortion during daily use.[76] In addition, the role of the electrolyte gel of FC-based OECT is worth mentioning, as it functions as a glue to bond the crossing fibers together and assist with their fixation.[105]

4. Recent advances of FCs in wearable electronics

Wearable electronics, particularly smart fabrics and textiles, have gained immense popularity in recent years due to their flexibility, comfort, and ease of integration into everyday clothing. FC-based devices have emerged as a crucial component in fabric and textile wearable electronics. These devices can be classified into five categories: mechanical sensing devices, chemical sensing devices, computing devices, display devices, and power supply devices. Each of these categories uses FC-based components as the core elements. For instance, mechanical sensing devices use FC-based resistors, capacitors, PENGs, and TENGs to monitor body movement, while power supply devices use FC-based PENGs, TENGs, supercapacitors, and solar cells to provide energy for the wearable system. In this article, we summarize the recent advances in FC-based devices in wearable electronics, highlighting their importance and potential for future developments. It is important to note that each type of FC-based device has unique application scenarios and limitations, which are provided in Table **S1** for more information.

4.1 FCs-based devices for wearable sensing

FC-based sensing systems are becoming increasingly important in daily life as they allow for continuous monitoring of various aspects of the wearer's health and activity. They have a

wide range of applications in areas such as fitness tracking, healthcare monitoring, and sports performance analysis. Additionally, wearable textile sensors have the potential to transform the way we interact with technology daily. FC-based sensor is a lightweight and comfortable front-end for wearable monitoring systems, which can be used for mechanical and chemical sensing applications, as shown in **Figure 4**.

4.1.1 FCs for mechanical sensing

FC-based resistors, capacitors, PENGs, and TENGs have the potential to detect mechanical stress and deformation, as well as non-contact distance.[28] By measuring real-time changes in resistance, capacitance, and piezo/triboelectric potential, these devices can detect pressure-induced deformations and provide valuable information on mechanical strain and stress.

4.1.1.1 FC-based resistors for mechanical sensing

When deformation occurs at the interlaced point of FC-based resistors, the contact resistance (R_c) and/or internal resistance (R_i) change with applied pressure. Metals, due to their excellent conductivity, are the dominant materials for the resistive layers of FC-based contact resistors. For example, Liu et al. used Cu nanoparticles as the resistive layer in an FC-based contact resistor sensor, deposited by polymer-assisted metal deposition (**Figure 4a**). The sensor exhibited excellent piezoresistive characteristics, including a wide strain range of up to 200%, a high gauge factor of 49.5 in 100% tensile strain, and high linearity (R^2 = 99.5%). The sensor's fiber structure allowed skin metabolites to be easily discharged into the air through water vaporing, ensuring its breathability.[97] Conducting polymers and carbon-based materials are also suitable for resistive layers, offering flexibility at the expense of lower conductivity. For example, Clevenger et al. used oxidative CVD-deposited PEDOT as the resistive layer in an FC-based contact resistor sensor (**Figure 4b**). The PEDOT layer exhibited good conformality and stability during 100 bending cycles, compared to the dip-coated PEDOT layer, which tore and separated from the fiber core easily after being bent. The sensor was integrated into

disposable masks to monitor respiratory rate and blood pressure.[9]

On-textile internal resistors offer several advantages over contact resistors, including fast response times, high sensitivity, and low power consumption. Wang et al. developed an ultra-stretchable FC-based internal resistor sensor that used silk carbides to generate cracks, as shown in **Figure 4c**. By carbonizing the silk through heat treatment under an inert atmosphere, cracks formed inside the silk carbides under stretching. The island microstructures within the cracks facilitated contact between the woven fibers, preventing conductive pathways from rupturing under large strains and contributing to the exceptional stretching properties of the FCs. With a high stretchability of up to 520% and a gauge factor of 5.8, the sensor was suitable for detecting a range of human motions and sounds.[102]

4.1.1.2 FC-based capacitors for mechanical sensing

Deformation at the interlaced point of FC-based capacitors causes a change in mutual capacitance (C_M) in response to applied pressure. Elastic insulating polymers are commonly used as dielectrics for FC-based capacitors due to their appropriate dielectric constant and high deformability. For instance, Lee et al. developed an FC-based capacitor sensor that utilized SBS with absorbed Ag nanoparticles as the electrode and dip-coated PDMS as the dielectric layer (**Figure 4d**).[103] In addition, a helical structure is widely adopted to form polymer dielectric layers, which can significantly enhance the sensitivity and stretchability of the woven structure. For example, You et al. reported an FC-based capacitor sensor that used electrospinning to spiral GO-dropped polyurethane nanofiber yarns around an elastic thread as the dielectric layer (**Figure 4e**). The sensor responded to a force of up to 5 N and exhibited excellent sensing properties, such as a detection limit down to 0.001 N, high sensitivity of 1.59 N^{-1}, and a short response time. They also fabricated a 64-pixel sensor array to measure the capacitance of each cross point and generate a two-dimensional pressure map under applied pressure.[40]

To enable touchless sensing, the fringe capacitance (C_F) between the FC-based capacitor and an approaching object can be utilized in addition to touch-type mutual capacitive sensing.

Guan et al. demonstrated this by reporting an FC-based capacitor sensor that can monitor both touch pressure and touchless object proximity. They used Ag-bacterial cellulose and PDMS as the electrode and dielectric layer, respectively (**Figure 4f**). The hierarchical porosity within the cellulose core ensured ultra-high touchless sensitivity of the sensor (0.19 cm^{-1}), and it was further integrated into a touchless textile keyboard.[10]

4.1.1.3 FC-based PENGs and TENGs for mechanical sensing

When the interlaced point of the FC-based PENGs is deformed, it generates a piezoelectric sensing voltage between two electrodes. PVDF and its copolymer P(VDF-TrFE) are commonly used as piezoelectric materials in FC-based PENGs due to their easy processing, high biocompatibility, good chemical resistance, and excellent mechanical strength. For instance, Park et al. developed an FC-based PENG sensor by attaching a piezoelectric PVDF film to a customized flexible printed circuit on the fiber (**Figure 4g**). The sensor was woven into fabrics to measure elbow flexion and extension by the output voltage. The flexural loading test showed favorable linearity between the peak-to-peak bending angle and the peak-to-peak voltage, as well as between the peak-to-peak voltages and the bending frequencies of the sensor, with an R-squared value greater than 0.99.[104]

The FC-based TENG operates by generating a periodic sensing pulse current through the closed circuit of the interlaced point when a reciprocating strain is applied. To create a washable FC-based TENG sensor for respiratory monitoring, Zhao et al. utilized industrial loom machines to weave Cu-coated polyethylene terephthalate (Cu-PET) fibers and PI-Cu-coated PET (PI-Cu-PET) fibers separately as the TENG electrodes (**Figure 4h**). When the sensor experiences tiny deformations induced by tapping or bending, the contact area at each cross-point of the FC changes, resulting in the efficient generation of TENG charges. The sensor achieved a significant maximum circuit current density of up to 15.50 mA m^{-2} and an open-circuit voltage of up to 4.98 V, making it suitable for respiratory monitoring.[14]

Furthermore, the power supply ability and sensitivity of FCs can be enhanced by

integrating PENGs with TENGs. He et al. developed an FC-based TENG sensor that was enhanced by a PENG through the interleaving of piezoelectric and triboelectric layers via high-temperature vulcanization (**Figure 4i**). The coordinated energy output of the TENG and PENG allowed for maximal capture of human-body motions, as shown by the output voltage and current that reached up to 600 V and 17 μA, respectively. The sensor was also attached conformally to the skin, and the corresponding output signal was generated when the tester walked.[46]

4.1.2 FCs for chemical sensing

Chemical sensing with FC-based OECTs is a popular approach, where the OECTs serve as the core sensing elements that convert the concentration of a substance into measurable signals, such as the source-drain current (I_{ds}). These sensors are used to monitor the concentration of various body surface organics and inorganics. When the substance being tested enters the electrolyte of the FC-based OECT, the de-doping of the electrical conducting polymer layers occurs, which changes the I_{ds} under a specific gate voltage (V_g). Carbon-based materials are often integrated with PPy to increase the electrochemical activity and sensitivity of the FC-based OECTs to organics. For instance, Zhang et al. developed an FC-based OECT lactate sensor using multiwalled CNTs doped PPy as the channel layer (**Figure 4j**). The presence of multiwalled CNTs induced a large area and dense growth of PPy nanowires, resulting in an ON/OFF ratio of up to 10^2 and excellent selectivity for lactate. The sensor was assembled with a Pt gate wire and woven into commercial cloths to form a wearable lactate sensor with a large linear response range from 1 nM to 1 mM and a quick response time. Similarly, the introduction of reduced GO can also facilitate large-area growth of high-quality PPy nanostructures. Wang et al. reported an FC-based OECT glucose sensor using PPy nanowires and reduced GO composites as the channel layer, which exhibited comparable sensing performance to the CNT-doped channel OECTs (**Figure 4k**).[105]

Moreover, FC-based OECTs can achieve a large ON/OFF ratio, fast response, and accurate

continuous sensing for inorganic materials such as metal ions. Wang et al. created an FC-based OECT lead ion sensor using PPy and polyvinyl alcohol (PVA)-co-PE nanofibers as the channel layer (**Figure 4l**). The sensor demonstrated excellent electrical performance with an ON/OFF ratio up to 10^4 at low drain-source voltages down to 2 V. The sensitivity reached 446 μA/dec to 10^{-5}-10^{-2} M Pb^{2+} solution. These sensors can also be used to detect other low-concentration metal ions, such as potassium, calcium, and aluminum ions.[106]

4.2 FCs for wearable computing

FC-based computing systems are a topic of great interest in research due to their capability of providing real-time, continuous, on-clothes data storage and analysis. State-of-the-art FC computing devices, as shown in **Figure 5**, utilize memristors and transistors for data storage and highly efficient edge computing, specifically in wearable electronics.[107] FC-based memristors, including interfacial and filamentary types, are used for operating resistive random-access memory (RRAM) and neuromorphic computing on wearable textiles, while FC-based transistors, such as OECTs and FETs, are used for conducting Boolean logic operations and neuromorphic computing on wearable electronics.

4.2.1 FC-based memristors for computing

Memristor RRAM is a promising technology for integrating computing and data storage due to its low power consumption, short response time, and cyclic switching stability.[108] FC-based memristors for RRAM use each fiber cross point as one bit of data storage. The high and low resistive states correspond to binary 1 and 0, respectively, reflecting the stored data through resistive state switching. Memristors also function as synaptic electronic devices for neuromorphic computing, a technology that imitates the behavior of biological neurons. Continuous current stimuli applied to the memristor cause its resistance to change, resulting in a higher postsynaptic current for subsequent stimuli than for initial ones. This phenomenon is divided into temporary short-term plasticity and persistent long-term plasticity, which are key components of mimicking the behavior of the brain neurons.[109]

4.2.1.1 FC-based interfacial memristors for computing

Hu et al. developed an FC-based memristor RRAM using rutile TiO_2 nanorods coated on carbon fibers as the memristive layer (**Figure 5a**). The memristor switched from a high to low resistance state when a positive voltage higher than the threshold (1.4 V) was applied, inducing significant width shrink of the depletion region and increasing the current passing through. The memristor exhibited a stabilized ON/OFF ratio of 10^2 without noticeable degradation after 1500 cycles.[21]

Wang et al. demonstrated resistive plasticity induced by vacancies in memristor synapses using $Ba_{0.6}Sr_{0.4}TiO_3$-coated carbon fibers as the memristive layer (**Figure 5b**). The fabricated memristor exhibited remarkable memory stability by retaining the low resistance state for 787 s during power outages and was cycled 10^3 times with consistent performance. The postsynaptic current continuously increased by sweeping the memristor from 0 V to + 1.5 V voltage for 10^3 cycles or by a programmable continuous pulse, indicating its potential as a synaptic electronic device for neuromorphic computing.[60]

4.2.1.2 FC-based filamentary memristors for computing

Jo et al. developed an FC-based electrochemical metallization-filamentary type memristor that utilized Al-coated threads with a native Al_2O_3 layer as the memristive layer. The two interlaced fibers acted as bit- and word-lines, respectively, in a 3×3 array RRAM prototype (**Figure 5c**). This RRAM demonstrated stable switching properties over 10^3 cycles with a 10^2 ON/OFF ratio under a 2-3 V bias.[20] Recently, FC-based electrochemical-metallization-type filamentary memristor synapses have been used to process complex physiological data and create effective artificial intelligence (AI) healthcare evaluating systems. Liu et al. developed a memristor synapse that used $CsPbBr_3$ perovskite as the memristive layer deposited by the electric field-induced assembly (**Figure 5d**). The memristor exhibited < 8% cycle-to-cycle variations under low setting voltages (0.16 V) and was woven into larger-scale arrays with high reproducibility from device to device. These arrays efficiently performed AI pattern recognition

tasks by inputting electrocardiogram signals into the memristor-based artificial neural network. During several learning processes, the weight values of each class displayed recognizable morphologies and waveforms, resulting in a total classification accuracy of up to 83%.

The FC-based thermal-chemical-filamentary type memristors have a potential mechanism for providing channels for the memristor filaments, notably, the soft breakdown of polymers. One such example is the work of Bae et al., who reported an FC-based TCM-type filamentary memristor RRAM. They used poly (ethylene glycol dimethacrylate) (pEGDMA) as the middle polymer for soft breakdown, resulting in carbon filaments with a 10 nm diameter that could control the resistive switching of the memristor (**Figure 5e**). When a voltage was applied, local soft breakdowns were triggered at the weakest point of the pEGDMA, causing the memristor to switch from a high resistance state to a low resistance state with an ON/OFF ratio of over 10^2 in 500 switching cycles. Moreover, this memristor achieved reliable operations on significantly curved surfaces, making it an ideal candidate for a skin-attached computing device. In addition, a half adder and other Boolean logic functional blocks were successfully realized using the memristor array.[111]

In addition, Park et al. presented an FC-based thermal-chemical-type filamentary memristor synapse utilizing electrochemically deposited reduced GO as the memristive layer, facilitating transitions from short-term plasticity to long-term plasticity (**Figure 5f**). When subjected to sufficient electric fields, the Joule heating effect caused the reduced GO to switch between low-conductive diamond forms and high-conductive graphitic forms, leading to changes in the memristor's resistance state. However, low-amplitude voltage pulses (< 2 V) were unable to generate enough Joule heat to induce a stable resistance change, causing the memristor's resistance state to rapidly decay to the initial state after terminating the low-amplitude voltage pulses. In contrast, high-amplitude voltage pulses (> 5 V) generated enough heat to induce a complete transformation of the reduced GO from the diamond form to the graphitic form, resulting in a significant increase in the memristor's conductivity for an

extended period even after the electrical pulse was removed (i.e., a long-term plasticity period).[64]

4.2.2 FC-based transistors for computing

Transistors offer several advantages over two-port devices. They have an additional gate port that allows the control of the drain-source channel conductance by applying a specific gate voltage. This feature not only increases cooperativity and controllability but also amplifies signal power and prevents circuit sneak path leakage.[109] Apart from their traditional use in Boolean logic operations, FC-based transistors also function as computing synapses due to their excitatory postsynaptic and paired-pulse facilitation properties.[112] These characteristics make them an excellent candidate for use in neuromorphic computing, where simulating the brain's synapses is a crucial part of developing artificial intelligence.

4.2.2.1 FC-based OECTs for computing

OECTs have proven to be effective not only in chemical sensing but also in Boolean operations. They offer high transconductance, large ON/OFF switching ratios, and low gate-voltage operation, making them an attractive option for computing. However, there are some drawbacks to using OECTs, such as relatively low switching speed, narrow dynamic range, and short level retention.[65] Additionally, the solution or gel electrolyte used in OECTs is not durable and incompatible with CMOS technologies, which could limit their mass production.[109]

Despite these limitations, significant progress has been made in developing operational logic circuits using FC-based OECTs. In 2007, p-type OECTs were constructed by coating conducting PEDOT:PSS film onto textile monofilaments (**Figures 5g-h**). The OECT channel gradually depleted and turned OFF from the normal ON state under a low gate voltage (~1.5V), with an ON/OFF ratio larger than 10^3.[19] Similarly, Yang et al. reported FC-based OECTs that used PEDOT:PSS and CNT as the channel layer and electrode layer, respectively (**Figure 5i**). They were able to construct a variety of transistor array circuits, including AND gates, OR gates,

and AND-OR gates, using the OECT array to demonstrate universal logic operations.[27]

4.2.2.2 FC-based FETs for computing

Compared to rigid metallic inorganics like IGZO, π-conjugated conducting organics offer greater flexibility and are more easily processed using solution-based techniques, making them ideal candidates for the channel layer of FC-based FETs.[113] FETs, like memristors, have shown potential in neuromorphic electronics for multi-bit memory with ultra-low energy consumption.[63] FC-based ferroelectric OFETs, in particular, offer greater adaptability to both CMOS and low-cost solution-based process techniques. The copolymer P(VDF-TrFE) is a preferred choice for the insulator layer of FC-based OFTEs due to its lightweight, highly scalable, and flexible properties. Kang et al. reported an FC-based ferroelectric OFET constructed on an Ag wire, utilizing a capillary tube dip-coating method to form nano-grained P(VDF-TrFE) insulator layers on the metal wire. The uniform surface topography of the P(VDF-TrFE) contributed to good switching stability (10^2 cycles), long retention (5×10^4 s), and low voltage operation (5 V) properties of the transistor. The OFET was further integrated into a fiber-based organic memory with ignorable performance degradation even under constant stretching loads.[71] Based on this OFET, Ham et al. developed an FC-based ferroelectric OFET synapse for large-scale wearable textile neuromorphic computing (**Figure 5j-k**). They formed a 10×10 fiber synapse array, where the output current of each synapse was added and propagated with small leakage. The array network achieved up to 70% recognition accuracy for electrocardiography signals and maintained accuracy even under bending and stretching conditions.[114]

4.3 FCs for wearable display

FC-based display systems enable users to receive visual information directly from their clothing, providing a convenient, hands-free way to access and display information without the need for a separate device, such as a smartphone or tablet. These systems are promising candidates for serving as the basic unit of wearable displays for real-time language and

emotional information exchange. FC-based lighting devices can be divided into two categories: electrical and non-electrical. Electrical FCs require a DC/AC electric field to excite light emission and use FC-based LEDs and electroluminescence devices as the core lighting elements. These electrical FCs are commonly used in displays. On the other hand, non-electrical FCs utilize mechanoluminescence to emit light and are often used in other applications. **Figure 6** shows an illustration of these two types of FC-based lighting devices.[74]

4.3.1 FC-based LEDs for display

FC-based LEDs, which have similar structures to commercial thin-film-based LEDs, are a promising technology. For example, Song et al. developed a fully addressable FC-based LED using fibers with rectangular sections as planar substrates for easy deposition of phosphorescent LED layers (**Figure 6a**). The LED featured a crossing architecture composed of one warp conductive fiber and one weft lighting fiber, enabling a two-dimensional, matrix-addressable LED network. The device was stable in both air and water, and its durability was improved by further encapsulation.[75] Similarly, Hwang et al. developed a bright, multicolor FC-based organic light-emitting diode (OLED) using a highly efficient dip-coating method for organics (**Figure 6b**). The OLED array achieved independent pixel control through a matrix-addressable scheme and successfully visualized letters and sentences on commercial clothes, demonstrating the potential for wearable and high-performance display systems.[76]

4.3.2 FC-based electroluminescence for display

The FC-based electroluminescence has simpler fabrication processes compared to multiple-layer FC-based LEDs. Additionally, the electroluminescent fiber only needs casual spatial contact with the connected fiber for sufficient luminous intensity, unlike the FC-based LEDs which require strictly close contact between fibers for stable lighting.[115] A study by Shi et al. developed a flexible and breathable display textile containing up to 5×10^5 FC-based electroluminescence units with a spacing of ~ 800 μm (**Figure 6c-d**). This display withstood repeated machine-washing and had a limited brightness deviation of only 8%, even under

bending, stretching, or pressing conditions. The luminance generated was 115.1 cd m^{-2} at 3.7 V μm^{-1} working voltage and 2000 Hz alternating frequency, with high current density (1.8 mA cm^{-2}) and low power consumption (363.1 μW). The display was integrated with an on-textile keyboard and a power supply as a powerful communication system, demonstrating its potential in intelligent fields such as instant communication and telemedicine.[12]

4.3.3 FC-based multifunctional display

The use of FC-based lighting devices, particularly those utilizing mechanoluminescence, has allowed for the development of multifunctional displays when combined with other devices. An example of this is seen in the work of Zhou et al., who created an FC-based mechanoluminescence-capacitor sensor that emits light when subjected to pressure (**Figure 6e-f**). The capacitor fiber was constructed by inserting a steel wire into a hollow spiral PDMS fiber containing ZnS:Cu phosphor. In this design, the steel wire, PDMS, and phosphor functioned as the electrode, dielectric layer, and light source, respectively, while commercial threads were woven with the capacitor fibers to transmit the pressure. The FC-based mechanoluminescence technology displayed high sensitivity and stability, maintaining a consistent luminescence response even after undergoing 100 loading-unloading cycling tests at 1 N.[79]

Nanogenerators, such as TENGs, can be combined with mechanoluminescence to create self-powered wearable sensors. For example, He et al. developed a fabric that incorporates both self-powered wearable mechanoluminescence and TENGs to collect mechanical energy while simultaneously monitoring and displaying real-time physiological signals (**Figure 6g**). To achieve this, they used a coil spring as an electrode that was uniformly coated with ZnS:Cu/PDMS phosphor, which enabled the fabric to have a large specific surface area for mechanical sensing and energy harvesting. As a result, the fabric was able to generate highly efficient lighting without the need for external circuitry.[116] This makes it well-suited for applications such as underwater monitoring, rescue, and information interaction (**Figure 6h**).[117]

4.4 FCs for wearable power supply

By integrating power sources directly into textiles, FC-based power supply systems provide greater comfort and portability for the wearer, making them more convenient than traditional bulky batteries. Additionally, they are designed to be flexible, durable, and lightweight, making them a practical and efficient solution for powering wearable electronics. To achieve these benefits, FC-based power supply systems are divided into two main categories: FC-based energy harvesting devices and FC-based energy storage devices, as shown in **Figure 7**. FC-based energy harvesting devices, such as piezoelectric nanogenerators (PENGs), triboelectric nanogenerators (TENGs), and solar cells, can transform mechanical or solar energy into electrical energy. FC-based energy storage devices, including supercapacitors, can store electrical power from other sources or energy harvesting devices, providing a reliable voltage or current output as needed. By integrating these power supply devices, it is possible to achieve high power density and capacity for combined power supply systems.[118]

4.4.1 FC-based PENGs and TENGs for energy harvesting

FC-based nanogenerators, such as PENGs and TENGs, have gained popularity for energy harvesting due to their lightweight, high instantaneous output, and universal availability. These nanogenerators can convert various types of mechanical energy generated by the user, including vibration, sliding, and displacement, into electrical energy. For piezoelectricity, Zhang et al. developed FC-based PENGs using barium titanate nanowires coated fibers (**Figure 7a**). The fiber was flexible, and the aligned barium titanate nanowires enhanced the piezoelectric properties as active materials. Interdigitated electrodes made of Cu wires woven with cotton threads were used, and the PENG was attached to elbows that bent periodically. The PENG generated a 1.9 V output voltage and 24 nA output current, sufficient to power a liquid-crystal display (**Figure 7b**).[47] For triboelectricity, Chen et al. developed FC-based TENGs using polytetrafluoroethylene and Cu as the core triboelectric layer and electrode, respectively (**Figure 7c**). These TENGs were woven with fiber-based solar cells using the shuttle-flying

method, and the power supply system was demonstrated to auxiliary charge a 2-mF commercial capacitor up to 2 V in 1 min.[82]

4.4.2 FC-based solar cells for energy harvesting

Powering wearable devices entirely by nanogenerators is challenging due to their reliance on body movement, which can be inconsistent and unstable in terms of output amplitude. Therefore, a sustainable, stable, and flexible solar-based power source could be a promising solution. Additionally, solar energy is a low-cost, clean, and renewable energy source. Zhang et al. developed an all-solid, metal compound-based FC-based solar cell that was woven in an interlaced manner, using ZnO-Mn coated polymer wire, CuI, and Cu wire as photoanode, hole-transfer layer, and counter electrode, respectively (**Figure 7d**). Under a light intensity of 100 mW cm^{-2}, the solar cell achieved an open circuit voltage of up to 4.6 V and a short-circuit current density of up to 7.8 mA cm^{-2}, with a solar cell unit efficiency of 1.3%.[81] Polymers have also been used as the functional materials of solar cells. Liu et al. reported an FC-based solar cell that achieved an open-circuit voltage and a short-circuit current of 0.83 V and 1.1 mA, respectively (**Figure 7e**). Using thermal-annealing PTB7:PC71BM and PEDOT:PSS coatings on ZnO layers as the active and hole transfer layers, the solar cell showed sufficient and stable power supply capability to power up a digital watch under solar irradiation.[83]

4.4.3 FC-based supercapacitors for energy storage

In addition to the plate FC-based capacitors used for mechanical sensing, large-capacity aqueous and gel electrolyte FC-based supercapacitors have also been developed for energy storage. For instance, Sun et al. developed an FC-based supercapacitor with hierarchical conducting structures by stacking two textile electrodes composed of a current collector grid and interlaced GO-modified fibers (**Figures 7f-h**). A PVA/H_3PO_4 gel electrolyte was then coated on the textile electrodes, and a separator was placed between them to create a single supercapacitor unit. Compared to single-fiber supercapacitors with only two parallel or twisted electrodes, this large-area (with an effective area of 100 cm^2) FC-based supercapacitor had high

energy storage performance, achieving a capacitance, power, and energy of 69.3 F, 80.7 mW, and 5.4 mWh, respectively.[119]

4.4.4 FC-based multimodal power supply

Various FC-based energy harvesting and storage devices offer an improved energy solution for smart wearables, providing greater convenience and comfort. However, ensuring both sustainability and stability of the power supply remains a significant challenge. PENGs and TENGs can convert the wearer's daily body motions into electrical energy, however, their output is alternating, and additional components and circuitry are needed to convert the AC output to DC output. Similarly, while solar cells can provide stable and continuous power during sunny days, their output is limited indoors. To overcome these challenges, a highly integrated FC-based energy system that includes nanogenerators, solar cells, supercapacitors, and necessary rectifier filter components is desirable. This system can perform multimodal energy harvesting, storage, and supply simultaneously, ensuring all-weather, stable, and high-efficiency textile-based power supply for wearables (**Figure 7i**).[120] One example of an FC-based combined power supply is the design by Gao et al. which includes both solar cells for photoelectric conversion and supercapacitor modules for energy storage (**Figure 7j**). During daylight hours, the solar cells charge the supercapacitors, resulting in an open-circuit voltage of 2 V and a short-circuit current of 0.14 mA. In the absence of sufficient sunlight, such as when operating indoors, at night, or in rainy weather, the electrical energy stored in the supercapacitor module can provide a stable and continuous power supply for the wearable device.[121] Moreover, FC-based combined batteries that can utilize both photovoltaic and chemical charging methods have the potential to achieve flexible and high-density power harvesting, storage, and supply for wearables (**Figure 7k-l**).[79]

5. Summary and outlook

In this review, we provide an overview of the recent advancements in FC-based devices, including their structure designs, material considerations, fabrication techniques, and

applications for wearable electronics. With the advancement of highly dense multifunctional integration and intelligence combinations, FC systems hold promising development trends for the future. However, despite their potential, many challenges still exist, such as feature size miniaturization, reliability, standardized evaluation, and marketing issues. These challenges currently limit the broader application of FC-based devices in various smart wearable fields (**Figure 8**). Nevertheless, the next-generation FC-based smart wearable systems have the potential to revolutionize many aspects of society, including medical, community, digital exchange, military, and environmental sectors.

5.1 Trends and challenges of FCs

5.1.1 Multifunctional integration

Multifunctional and highly integrated wearable electronics represent an important direction for the development of wearable technology. By combining multiple functions, such as sensing, computing, and display, into a single device, these wearables offer enhanced capabilities and a more seamless user experience. Multifunctional FC textiles can perform multiple functions in a single fabric. Recent research has focused on integrating different FC-based devices, such as capacitors, luminescent devices, and nanogenerators, to enhance the functionality and performance of wearable textile electronics.[79] Recently, Yang et al. reported a high-density FC-based integrated circuit (IC) that can perform complex operations on the same processing power level as industrial systems.[27] However, current FC-based systems still require non-textile modules to perform auxiliary tasks. For instance, Xu et al. reported an integrated computing textile composed of FC-based memristors, fiber-based batteries, and LEDs, but external microcontrollers were needed for timing control signals.[26] To develop truly independent FC-based systems, more functions, such as multiple sensing, high-speed computing, high-quality display, control system, information transmission, and power supply, should be integrated. By doing so, wearable electronics would be more efficient and user-friendly, and improve the overall user experience.

5.1.2 Intelligence

The integration of AI techniques can significantly enhance the computing power and analysis capabilities of FC-based systems for wearable electronics. On-chip AI operations and off-chip AI analysis have already been widely used in smart wearable systems. Recent studies have explored innovative ways to integrate AI chips into fibers through thermal drawing, which has the potential to improve the computing power of a single FC fiber.[122] However, the current on-chip AI computing power of FC systems is quite limited due to the insufficient integration of devices. As a result, they are only suitable for processing small batches of standardized data with low accuracy. Improving device performance, enlarging array scale and density, and enabling more AI algorithms could be the solutions for developing FC-based AI systems with more substantial computing power. Off-chip AI analysis is also widely used in current FC-based sensors for wearable electronics. The data collected by dense wearable sensors, such as smart gloves, is transmitted to PC terminals and processed by an artificial neural network for analysis and pre-evaluation.[123] For example, Luo et al. developed an FC-based tactile learning glove that captures more than a million tactile frames of diverse human-environment interactions, demonstrating that off-chip AI-powered sensing gloves can classify sitting poses, motions, and other interactions of humans.[124] Increasing the number and density of sensing elements is the prerequisite for FC-based sensors to realize large-scale data collection and more accurate off-chip AI analysis.

5.1.3 Size miniaturization

The integration of multifunctional and AI-based FC devices in wearable electronics demands a high density of devices on fabrics, which necessitates miniaturization. Larger FC-based devices may hamper the flexibility and wearing comfort of the textile, making device miniaturization a prerequisite. However, many current cleanroom fabricating techniques are unsuitable for fibers with highly curved surfaces. One solution is to use fibers with flat surfaces for device fabrication.[125] Alternatively, developing more advanced, fiber-compatible

fabrication techniques such as nanoimprinting[126] and curved-surface lithography[127] is a promising approach toward the miniaturization of FC-based devices. Although these techniques are not yet fully mature, they have the potential to realize more lightweight, miniaturized, and integrated FC-based systems, enhancing the user experience of wearable electronics.

5.1.4 Circuitry reliability

To ensure the reliability of the global circuitry of FCs, several measures need to be taken. For highly integrated FC systems, damage to any part can lead to serious failure of the wearables. The following measures may be helpful in improving FC's global circuitry reliability. Firstly, poor contact, dislocation, and displacement may occur at the intersections between fibers and induce device failures. To avoid these issues, fixation and encapsulation are necessary to keep stable connections of FC's electronic wiring point. In addition, key parts of the FCs need strict sealing to avoid leakage during daily washing. Secondly, optimizing the circuit layout is also an important method to improve the reliability of the FC system. This involves ensuring that each FC-based device is positioned correctly, while also making sure that the textile as a whole is easy to spin, weave, and knit. Additionally, since most FC-based devices require an electrical power supply, it is essential to develop fibrous batteries with large capacity and lightweight that can support the stable operation of the FC system. Thirdly, the electrical properties of specific materials, including some conducting polymers, could degrade rapidly under normal room conditions. Therefore, choosing materials with good stability and durability as the primary.

5.1.5 Standardized evaluation

The lack of unified performance evaluation criteria for FC-based devices during the initial development phase is a common challenge. Various factors, such as ambient temperature and humidity, can affect the performance and stability of the devices, making it crucial to establish standardized testing conditions. Additionally, there are numerous performance indicators for these devices, such as energy consumption, ON/OFF ratio, switching speed, and stability for

memristors. To ensure optimal working performance and promote comprehensive design, system-level optimization, and batch fabrication of FC-based systems, it is necessary to establish a standardized evaluation system with clear performance indicators. Such a system would help overcome the challenges associated with device evaluation and enable faster adoption of these devices in the development of high-performance wearable electronics

5.1.6 Marketing

The commercial success of FC-based wearable electronics depends not only on their electronic performance but also on their environmental friendliness, power efficiency, and user comfort. In terms of environmental friendliness, there is a need to reduce the proportion of heavy metallic materials used in FC-based devices and increase the use of degradable and bio-friendly materials. This is especially important given that wearable electronics are daily-used devices that have the potential to generate a significant amount of electronic waste. To achieve high power efficiency and low cost, there is a need to optimize the design of FCs and reduce the power consumption of the device as much as possible without compromising performance. Finally, since wearable electronics are meant to be worn for prolonged periods, ergonomics should be a key consideration in the design of FCs. The devices should be comfortable to wear and not cause any discomfort or foreign body sensations to the user.[128] Meeting these market demands will be crucial in the widespread adoption of FC-based wearable electronics.

5.2 Future trends

5.2.1 Reshaping future medical

Thanks to the soft and breathable characteristics of FC fabrics, it is possible to integrate various FC-based healthcare devices into smart textiles, which can be sewn into clothing, hospital bed linings, and wheelchair cushions to provide more comfortable medical-grade monitoring (**Figure 9a**). This change can undoubtedly improve the care of long-term bedridden patients. Furthermore, home healthcare is an essential complement to hospital treatment. While hospitals mainly focus on surgical treatment and nursing for serious injuries and diseases, long-

term body recovery, especially for chronic and elderly patients, needs to be carried out under the supervision of family doctors. Compared to existing commercial home medical testing equipment, FC-based healthcare devices have the potential to offer automatic, continuous, and convenient monitoring of basic health data such as blood pressure, blood sugar, and heart rate (**Figure 9b**). These data can be transmitted to the family doctor or hospital, which can then be used to formulate the next-step medical plan.

5.2.2 Reshaping future community

FC-based systems are versatile and intelligent textiles with the potential to transform community life in the future. The integration of various FC-based sensors into sports clothing can provide valuable data to monitor individual exercise and assist in athlete training, leading to more reasonable training plans (**Figure 9c**). Furthermore, FC-based devices could benefit individuals with disabilities, such as congenital or disease-induced deafness and muteness, which may result in the long-term social absence and mental illness. FC-based displays have the potential to help these individuals express themselves more fluently, allowing them to input their needs and intentions through mobile phones, wearable wristband keyboards, and even brain-computer interfaces. The information can be shown on FC-based display textiles for others to know (**Figure 9d**). Additionally, FC systems could establish a personal data port and link each person's information node into a powerful 5G/6G-based network, including personal information like health data, exercise data, and language data, which can be collected by FC-based systems.

5.2.3 Reshaping future digital exchange

In addition to being stored locally, the data collected can also be transmitted to nearby terminals or cloud storage for backup or further analysis (**Figure 9e**). It is important to note that the reshaped digital exchange model has both positive and negative aspects. On the positive side, it provides data support for future medical and healthcare, convenience for people with disabilities, and a powerful channel for human-human and human-machine information

interaction. However, on the negative side, it can also pose serious security risks and infringe on human rights, such as personal data breaches.

5.2.4 Reshaping future defense

FCs have various military applications, including aiding in military training, combat situations, and anti-terrorism efforts. Like healthcare devices, FC-based sensors can automatically and continuously monitor the physical performance data of soldiers to optimize their training plans. Additionally, FC-based power supply devices can provide energy for different military equipment and maintain their normal functioning, enhancing the long-range attack capabilities of individual soldiers. Moreover, effective verbal communication may not be possible in battlefield conditions, such as when entering a room to rescue hostages, where soldiers need to maintain silence to avoid revealing their position. In such scenarios, FC-based displays can be used to display simple commands on the uniform, facilitating timely communication between soldiers (**Figure 9f**). It is worth noting that while FC technology has significant potential in the defence sector, its use should be carefully considered considering potential security risks and ethical concerns.

5.2.5 Reshaping future environment

FC-based power supply devices offer a promising solution for powering wearable devices using renewable energy sources, such as user movement and solar energy, instead of relying on traditional power plants. In an ideal scenario, each user becomes a small, distributed, and self-sufficient power source, thereby reducing their carbon footprint and contributing to environmental sustainability goals (**Figures 9g-h**). For instance, FC-based sensors can harness kinetic energy from the user's movement and convert it into electrical energy to power the device. Additionally, solar cells integrated into FC fabrics can capture sunlight during the day and store the energy in supercapacitors for use at night. This approach enables wearables to become all-self-powered functional bodies, achieving energy self-sufficiency. However, it is essential to keep the power consumption of the devices to a minimum to achieve this goal.

Acknowledgements

This work was supported by the Singapore Ministry of Education Academic Research Fund Tier 2 (MOE2019-T2-2-127 and MOE-T2EP50120-0002), the Singapore Ministry of Education Academic Research Fund Tier 1 (RG62/22), Suzhou Institute of Nano-Tech and Nano-Bionics, Chinese Academy of Sciences (Start-up grant E1552102), A*STAR under AME IRG (A2083c0062), and A*STAR under IAF-ICP Programme I2001E0067 and the Schaeffler Hub for Advanced Research at NTU. This work was also supported by NTU-PSL Joint Lab collaboration. This work was supported by the Shenzhen Basic Research grants GJHZ20200731095601004, Guangdong Basic and Applied Basic Research Foundation (2023A1515030113), and Youth Innovation Promotion Association, Chinese Academy of Sciences, China (2023375). This work was supported by the IDMxS (Institute for Digital Molecular Analytics and Science) by the Singapore Ministry of Education under the Research Centres of Excellence scheme.

Received: (will be filled in by the editorial staff)

Revised: (will be filled in by the editorial staff)

Published online: (will be filled in by the editorial staff)

References

[1] Y. Zheng, N. Tang, R. Omar, Z. Hu, T. Duong, J. Wang, W. Wu, H. Haick, *Adv. Funct. Mater.* **2021**, 31, 51.

[2] K. Bayoumy, M. Gaber, A. Elshafeey, O. Mhaimeed, E. Dineen, F. Marvel, S. Martin, E. Muse, M. Turakhia, K. Tarakji, M. Elshazly, *Nat. Rev. Cardiol.* **2021**, 18, 581-599.

[3] K. Singha, J. Kumar, P. Pandit, *Mater. Today* **2019**, 16, 1518-1523.

[4] G. Lee, H. Moon, H. Kim, G. Lee, W. Kwon, S. Yoo, D. Myung, S. Yun, Z. Bao, S. Hahn, *Nat. Rev. Mater.* **2020**, 5, 149-165.

[5] H. Yuk, B. Lu, X. Zhao, *Chem. Soc. Rev.* **2019**, 48, 1642-1667.

[6] W. Yan, C. Dong, Y. Xiang, S. Jiang, A. Leber, G. Loke, W. Xu, C. Hou, S. Zhou, M. Chen, R. Hu, P. Shum, L. Wei, X. Jia, F. Sorin, X. Tao, G. Tao, *Mater. Today* **2020**, 35, 168-194.

[7] A. Rajappan, B. Jumet, R. Shveda, C. Decker, Z. Liu, T. Yap, V. Sanchez, D. Preston, *Proc. Natl. Acad. Sci.* **2022**, 119, e2202118119.

[8] A. Libanori, G. Chen, X. Zhao, Y. Zhou, J. Chen, *Nat. Electron.* **2022**, 5, 142-156.

[9] M. Clevenger, H. Kim, H. Song, K. No, S. Lee, *Sci. Adv.* **2021**, 7, eabj8958.

[10] F. Guan, Y. Xie, H. Wu, Y. Meng, Y. Shi, M. Gao, Z. Zhang, S. Chen, Y. Chen, H. Wang, Q. Pei, *ACS Nano* **2020**, 14, 15428-15439.

[11] X. Qing, Y. Wang, Y. Zhang, X. Ding, W. Zhong, D. Wang, W. Wang, Q. Liu, K. Liu, M. Li, Z. Lu, *ACS Appl. Mater. Interfaces* **2019**, 11, 13105-13113.

[12] X. Shi, Y. Zuo, P. Zhai, J. Shen, Y. Yang, Z. Gao, M. Liao, J. Wu, J. Wang, X. Xu, Q. Tong, B. Zhang, B. Wang, X. Sun, L. Zhang, Q. Pei, D. Jin, P. Chen, H. Peng, *Nature* **2021**, 591, 240-245.

[13] L. Wang, X. Fu, J. He, X. Shi, T. Chen, P. Chen, B. Wang, H. Peng, *Adv. Mater.* **2020**, 32, e1901971.

[14] Z. Zhao, C. Yan, Z. Liu, X. Fu, L. Peng, Y. Hu, Z. Zheng, *Adv. Mater.* **2016**, 28, 10267-10274.

[15] C. Chen, L. Chen, Z. Wu, H. Guo, W. Yu, Z. Du, Z. Wang, *Mater. Today* **2020**, 32, 84-93.

[16] G. Tian, L. Zhan, J. Deng, H. Liu, J. Li, J. Ma, X. Jin, Q. Ke, C. Huang, *Chem. Eng. J* **2021**, 425, 130682.

[17] T. Yang, W. Wang, H. Zhang, X. Li, J. Shi, Y. He, Q. Zheng, Z. Li, H. Zhu, *ACS Nano* **2015**, 9, 10867-10875.

[18] W. Weng, Q. Sun, Y. Zhang, H. Lin, J. Ren, X. Lu, M. Wang, H. Peng, *Nano Lett.* **2014**, 14, 3432-3438.

[19] M. Hamedi, R. Forchheimer, O. Inganäs, *Nat. Mater.* **2007**, 6, 357-362.

[20] A. Jo, Y. Seo, M. Ko, C. Kim, H. Kim, S. Nam, H. Choi, C. Hwang, M. Lee, *Adv. Funct.* **2017**, 27, 1605593.

[21] S. Hu, J. Yue, C. Jiang, X. Tang, X. Huang, Z. Du, C. Wang, *Ceram. Int.* **2019**, 45,

10182-10186.

[22] Z. Wang, T. Wu, Z. Wang, T. Zhang, M. Chen, J. Zhang, L. Liu, M. Qi, Q. Zhang, J. Yang, W. Liu, H. Chen, Y. Luo, L. Wei, *Nat. Commun.* **2020**, 11, 3842.

[23] T. Nezakati, A. Seifalian, A. Tan, A. Seifalian, *Chem. Rev.* **2018**, 118, 6766-6843.

[24] G. Zhang, X. Liu, L. Wang, H. Fu, *J. Mater. Chem. A* **2022**, 10, 9277-9307.

[25] F. Mokhtari, G. Spinks, C. Fay, Z. Cheng, R. Raad, J. Xi, J. Foroughi, *Adv. Mater. Technol.* **2020**, 5, 4.

[26] X. Xu, X. Zhou, T. Wang, X. Shi, Y. Liu, Y. Zuo, L. Xu, M. Wang, X. Hu, X. Yang, J. Chen, X. Yang, L. Chen, P. Chen, H. Peng, *Angew. Chem. Int. Ed. Engl.* **2020**, 59, 12762-12768.

[27] Y. Yang, X. Wei, N. Zhang, J. Zheng, X. Chen, Q. Wen, X. Luo, C. Y. Lee, X. Liu, X. Zhang, J. Chen, C. Tao, W. Zhang, X. Fan, *Nat. Commun.* **2021**, 12, 4876.

[28] S. Seyedin, P. Zhang, M. Naebe, S. Qin, J. Chen, X. Wang, J. Razal, *Mater. Horizons* **2019**, 6, 219-249.

[29] Z. Liu, T. Zhu, J. Wang, Z. Zheng, Y. Li, J. Li, Y. Lai, *Nanomicro. Lett.* **2022**, 14, 61.

[30] K. Qi, H. Wang, X. You, X. Tao, M. Li, Y. Zhou, Y. Zhang, J. He, W. Shao, S. Cui, *J Colloid Interface Sci.* **2020**, 561, 93-103.

[31] J. Ge, L. Sun, F. Zhang, Y. Zhang, L. Shi, H. Zhao, H. Zhu, H. Jiang, S. Yu, *Adv. Mater.* **2016**, 28, 722-728.

[32] J. Deng, W. Zhuang, L. Bao, X. Wu, J. Gao, B. Wang, X. Sun, H. Peng, *Carbon* **2019**, 149, 63-70.

[33] X. Liao, Q. Liao, Z. Zhang, X. Yan, Q. Liang, Q. Wang, M. Li, Y. Zhang, *Adv. Funct. Mater.* **2016**, 26, 3074-3081.

[34] T. Yamada, Y. Hayamizu, Y. Yamamoto, Y. Yomogida, A. Najafabadi, D. Futaba, K. Hata, *Nat. Nanotechnol.* **2011**, 6, 296-301.

[35] X. Liu, D. Liu, J. Lee, Q. Zheng, X. Du, X. Zhang, H. Xu, Z. Wang, Y. Wu, X. Shen, J. Cui, Y. Mai, J. Kim, *ACS Appl. Mater. Interfaces* **2019**, 11, 2282-2294.

[36] S. Wang, H. Ning, N. Hu, Y. Liu, F. Liu, R. Zou, K. Huang, X. Wu, S. Weng, Alamusi, *Adv. Mater. Interface* **2019**, 7, 1901507.

[37] M. Zhang, C. Wang, H. Wang, M. Jian, X. Hao, Y. Zhang, *Adv. Funct. Mater.* **2017**, 27,

1604795.

[38] B. Yin, Y. Wen, T. Hong, Z. Xie, G. Yuan, Q. Ji, H. Jia, *ACS Appl. Mater. Interfaces* **2017**, 9, 32054-32064.

[39] J. Heo, J. Eom, Y. Kim, S. Park, *Small* **2018**, 14, 3.

[40] X. You, J. He, N. Nan, X. Sun, K. Qi, Y. Zhou, W. Shao, F. Liu, S. Cui, *J. Mater. C* **2018**, 6, 12981-12991.

[41] R. Wu, L. Ma, C. Hou, Z. Meng, W. Guo, W. Yu, R. Yu, F. Hu, X. Liu, *Small* **2019**, 15, e1901558.

[42] S. Takamatsu, T. Kobayashi, N. Shibayama, K. Miyake, T. Itoh, *Sens. Actuator A Phys.* **2012**, 184, 57-63.

[43] P. Jiao, *Nano Energy* **2021** 88, 106227.

[44] Z. Dai, N. Wang, Y. Yu, Y. Lu, L. Jiang, D. Zhang, X. Wang, X. Yan, Y. Long, *ACS Appl. Mater. Interfaces* **2021**, 13, 44234-44242.

[45] K. Dong, X. Peng, Z. Wang, *Adv. Mater.* **2020**, 32, e1902549.

[46] J. He, S. Qian, X. Niu, N. Zhang, J. Qian, X. Hou, J. Mu, W. Geng, X. Chou, *Nano Energy* **2019**, 64, 103933.

[47] M. Zhang, T. Gao, J. Wang, J. Liao, Y. Qiu, Q. Yang, H. Xue, Z. Shi, Y. Zhao, Z. Xiong, L. Chen, *Nano Energy* **2015**, 13, 298-305.

[48] F. Mokhtari, Z. Cheng, R. Raad, J. Xi, J. Foroughi, *J Mater. Chem. A* **2020**, 8, 9496-9522.

[49] Y. Zhou, J. He, H. Wang, K. Qi, N. Nan, X. You, W. Shao, L. Wang, B. Ding, S. Cui, *Sci. Rep.* **2017**, 7, 12949

[50] J. Ryu, J. Kim, J. Oh, S. Lim, J. Sim, J. Jeon, K. No, S. Park, S. Hong, *Nano Energy* **2019**, 55, 348-353.

[51] S. Mahapatra, P. Mohapatra, A. Aria, G. Christie, Y. Mishra, S. Hofmann, V. Thakur, *Adv. Sci.* **2021**, 8, e2100864.

[52] Z. L. Wang, *Adv. Energy Mater.* **2020**, 10, 2000137.

[53] Z. Zhao, Q. Huang, C. Yan, Y. Liu, X. Zeng, X. Wei, Y. Hu, Z. Zheng, *Nano Energy* **2020**, 70, 104528.

[54] C. Ning, K. Dong, R. Cheng, J. Yi, C. Ye, X. Peng, F. Sheng, Y. Jiang, Z. Wang, *Adv.*

Funct. Mater. **2020**, 31, 2006679.

[55] M. Chen, Z. Wang, Q. Zhang, Z. Wang, W. Liu, M. Chen, L. Wei, *Nat. Commun.* **2021**, 12, 1416.

[56] Y. Yang, L. Xie, Z. Wen, C. Chen, X. Chen, A. Wei, P. Cheng, X. Xie, X. Sun, *ACS Appl. Mater. Interfaces* **2018**, 10, 42356-42362.

[57] Y. Li, Z. Wang, R. Midya, Q. Xia, J. Yang, *J Phys. D Appl. Phys* **2018**, 51, 503002.

[58] S. Kim, J. Han, H. Kim, S. Kim, H. Jang, *Adv. Mater. Technol.* **2018**, 3, 1800457.

[59] B. Choi, J. Zhang, K. Norris, G. Gibson, K. Kim, W. Jackson, M. Zhang, Z. Li, J. Yang, R. Williams, *Adv. Mater.* **2016**, 28, 356-362.

[60] Z. Wang, J. Yue, C. Jiang, I. Abrahams, Y. Yu, Y. Li, Z. Du, X. Huang, L. Li, G. Wang, H. Zhou, *Ceram. Int.* **2020**, 46, 21569-21577.

[61] D. Kim, B. Jeon, Y. Lee, D. Kim, Y. Cho, S. Kim, *Appl. Phys. Lett.* **2022**, 121, 010501.

[62] I. Valov, R. Waser, J. Jameson, M. Kozicki, *Nanotechnology* **2011**, 22, 25.

[63] C. Wang, Y. Li, Y. Wang, X. Xu, M. Fu, Y. Liu, Z. Lin, H. Ling, P. Gkoupidenis, M. Yi, L. Xie, F. Yan, W. Huang, *J Mater. Chem. C* **2021**, 9, 11464-11483.

[64] Y. Park, M. Park, J. Lee, *Adv. Funct. Mater* **2018**, 28, 1804123.

[65] J. Rivnay, S. Inal, A. Salleo, R. Owens, M. Berggren, G. Malliaras, *Nat. Rev. Mater.* **2018**, 3, 2.

[66] M. Ghittorelli, L. Lingstedt, P. Romele, N. Craciun, Z. Kovacs-Vajna, P. Blom, F. Torricelli, *Nat Commun* **2018**, 9, 1441

[67] B. Wang, A. Thukral, Z. Xie, L. Liu, X. Zhang, W. Huang, X. Yu, C. Yu, T. Marks, A. Facchetti, *Nat Commun* **2020**, 11, 2405.

[68] C. Muller, M. Hamedi, R. Karlsson, R. Jansson, R. Marcilla, M. Hedhammar, O. Inganas, *Adv. Mater.* **2011**, 23, 898-901.

[69] W. Shi, Y. Guo, Y. Liu, *Adv. Mater.* **2020**, 32, e1901493.

[70] J. Heo, T. Kim, S. Ban, D. Kim, J. Lee, J. Jur, M. Kim, Y. Kim, Y. Hong, S. Park, *Adv. Mater.* **2017**, 29, 1701822.

[71] M. Kang, S. Lee, S. Jang, S. Hwang, S. Lee, S. Bae, J. Hong, S. Lee, K. Jeong, J. Lim, T. Kim, *ACS Appl. Mater. Interfaces* **2019**, 11, 22575-22582.

[72] S. Yoon, K. Lee, H. Cha, D. Seong, M. Um, J. Byun, Y. Oh, J. Oh, W. Lee, J. Lee, *Sci.*

Rep. **2015**, 5, 16366.

[73] G. Prunet, F. Pawula, G. Fleury, E. Cloutet, A. Robinson, G. Hadziioannou, A. Pakdel, *Materials Today Physics* **2021**, 18, 100402.

[74] S. Kwon, Y. Hwang, M. Nam, H. Chae, H. Lee, Y. Jeon, S. Lee, C. Kim, S. Choi, E. Jeong, K. Choi, *Adv. Mater.* **2020**, 32, e1903488.

[75] Y. Song, J. Kim, H. Cho, Y. Son, M. Lee, J. Lee, K. Choi, S. Lee, *ACS Nano* **2020**, 14, 1133-1140.

[76] Y. Hwang, S. Kwon, J. Shin, H. Kim, Y. Son, H. Lee, B. Noh, M. Nam, K. Choi, *Adv. Funct. Mater.* **2021**, 31, 2009336.

[77] L. Wang, L. Xiao, H. Gu, H. Sun, *Adv. Opt. Mater.* **2019**, 7, 1801154.

[78] Y. Zhuang, R. Xie, *Adv. Mater.* **2021**, 33, e2005925.

[79] N. Zhang, F. Huang, S. Zhao, X. Lv, Y. Zhou, S. Xiang, S. Xu, Y. Li, G. Chen, C. Tao, Y. Nie, J. Chen, X. Fan, *Matter* **2020**, 2, 1260-1269.

[80] M. Hatamvand, E. Kamrani, M. Lira-Cantú, M. Madsen, B. Patil, P. Vivo, M. Mehmood, A. Numan, I. Ahmed, Y. Zhan, *Nano Energy* **2020**, 71, 104609.

[81] N. Zhang, J. Chen, Y. Huang, W. Guo, J. Yang, J. Du, X. Fan, C. Tao, *Adv. Mater.* **2016**, 28, 263-269.

[82] J. Chen, Y. Huang, N. Zhang, H. Zou, R. Liu, C. Tao, X. Fan, Z. Wang, *Nat. Energy* **2016**, 1, 1-8.

[83] P. Liu, Z. Gao, L. Xu, X. Shi, X. Fu, K. Li, B. Zhang, X. Sun, H. Peng, *J Mater. Chem. A* **2018**, 6, 19947-19953.

[84] A. Ugale, G. Umarji, S. Jung, N. Deshpande, W. Lee, H. Cho, J. Yoo, Sens. Actuators B Chem. 2020, 308, 127690.

[85] J. Kim, W. Lee, Y. Kang, S. Cho, K. Jang, Carbon 2018, 133, 293-299.

[86] S. Lee, W. Eom, H. Shin, R. Ambade, J. Bang, H. Kim, T. Han, ACS Appl. Mater. Interfaces 2020, 12, 10434-10442.

[87] Y. Li, J. Zhu, H. Cheng, G. Li, H. Cho, M. Jiang, Q. Gao, X. Zhang, Adv. Mater. Technol. 2021, 6, 2100410.

[88] H. Sim, C. Choi, S. Kim, K. Kim, C. Lee, Y. Kim, X. Lepro, R. Baughman, S. Kim, Sci. Rep. 2016, 6, 35153.

[89] C. Yang, S. Cheng, X. Yao, G. Nian, Q. Liu, Z. Suo, Adv. Mater. 2020, 32, e2005545.

[90] H. Kim, H. Kang, D. Hwang, H. Lim, B. Ju, J. Lim, Adv. Funct. Mater. 2016, 26, 2706-2714.

[91] M. Hamedi, L. Herlogsson, X. Crispin, R. Marcilla, M. Berggren, O. Inganas, Adv. Mater. 2009, 21, 573-577.

[92] H. Lin, W. Weng, J. Ren, L. Qiu, Z. Zhang, P. Chen, X. Chen, J. Deng, Y. Wang, H. Peng, Adv. Mater. 2014, 26, 1217-1222.

[93] G. Loke, W. Yan, T. Khudiyev, G. Noel, Y. Fink, Adv. Mater. 2020, 32, e1904911.

[94] M. Chen, Z. Wang, K. Li, X. Wang, L. Wei, Adv. Fiber Mater. 2021, 3, 1-13.

[95] X. Lu, H. Qu, M. Skorobogatiy, Sci. Rep. 2017, 7, 2907.

[96] V. Vijayakumar, B. Anothumakkool, S. Kurungot, M. Winter, J. Nair, Energy & Environ. Sci. 2021, 14, 2708-2788.

[97] Z. Liu, Y. Zheng, L. Jin, K. Chen, H. Zhai, Q. Huang, Z. Chen, Y. Yi, M. Umar, L. Xu, G. Li, Q. Song, P. Yue, Y. Li, Z. Zheng, Adv. Funct. Mater. 2021, 31, 2007622.

[98] S. An, H. Jo, D. Kim, H. Lee, B. Ju, S. Al-Deyab, J. Ahn, Y. Qin, M. Swihart, A. Yarin, S. Yoon, Adv. Mater. 2016, 28, 7149-7154.

[99] Y. Ting, J. Chen, C. Huang, T. Huang, C. Hsieh, W. Wu, Small 2018, 14, 1703153.

[100] J. Yang, Q. Zhang, Z. Wang, Z. Wang, L. Kang, M. Qi, M. Chen, W. Liu, W. Gong, W. Lu, P. P. Shum, L. Wei, Adv. Energy Mater. 2020, 10, 2001064.

[101] S. Seyedin, J. Razal, P. Innis, A. Jeiranikhameneh, S. Beirne, G. Wallace, *ACS Appl. Mater. Interfaces* **2015**, 7, 21150-21158.

[102] C. Wang, X. Li, E. Gao, M. Jian, K. Xia, Q. Wang, Z. Xu, T. Ren, Y. Zhang, *Adv. Mater.* **2016**, 28, 6640-6648.

[103] J. Lee, H. Kwon, J. Seo, S. Shin, J. Koo, C. Pang, S. Son, J. Kim, Y. Jang, D. Kim, T. Lee, *Adv. Mater.* **2015**, 27, 2433-2439.

[104] C. Park, H. Kim, Y. Cha, *Appl. Sci.* **2020**, 10.

[105] Y. Wang, X. Qing, Q. Zhou, Y. Zhang, Q. Liu, K. Liu, W. Wang, M. Li, Z. Lu, Y. Chen, D. Wang, *Biosens. Bioelectron.* **2017**, 95, 138-145.

[106] Y. Wang, Z. Zhou, X. Qing, W. Zhong, Q. Liu, W. Wang, M. Li, K. Liu, D. Wang, *Anal. Bioanal. Chem.* **2016**, 408, 5779-5787.

[107] H. Park, Y. Lee, N. Kim, D. Seo, G. Go, T. Lee, *Adv. Mater.* **2020**, 32, e1903558.

[108] A. Mehonic, A. Sebastian, B. Rajendran, O. Simeone, E. Vasilaki, A. Kenyon, *Adv. Intell. Syst.* **2020**, 2, 2000085.

[109] M. Kim, Y. Park, I. Kim, J. Lee, *iScience* **2020**, 23, 101846.

[110] Y. Liu, X. Zhou, H. Yan, Z. Zhu, X. Shi, Y. Peng, L. Chen, P. Chen, H. Peng, *Adv. Funct. Mater.* **2022**, 32, 2201510.

[111] H. Bae, B. Jang, H. Park, S. Jung, H. Lee, J. Park, S. Jeon, G. Son, I. Tcho, K. Yu, S. Im, S. Choi, Y. Choi, *Nano Lett.* **2017**, 17, 6443-6452.

[112] D. Liu, Q. Shi, S. Dai, J. Huang, *Small* **2020**, 16, e1907472.

[113] R. Owyeung, T. Terse-Thakoor, H. Nejad, M. Panzer, S. Sonkusale, *ACS Appl.Mater. Interfaces* **2019**, 11, 31096-31104.

[114] S. Ham, M. Kang, S. Jang, J. Jang, S. Choi, T. Kim, G. Wang, *Sci. Adv.* **2020**, 6, eaba1178.

[115] G. Liang, M. Yi, H. Hu, K. Ding, L. Wang, H. Zeng, J. Tang, L. Liao, C. Nan, Y. He, C. Ye, *Adv. Electron. Mater.* **2017**, 3, 1700401.

[116] M. He, W. Du, Y. Feng, S. Li, W. Wang, X. Zhang, A. Yu, L. Wan, J. Zhai, *Nano Energy* **2021**, 86, 106058.

[117] W. Yang, W. Gong, W. Gu, Z. Liu, C. Hou, Y. Li, Q. Zhang, H. Wang, *Adv. Mater.* **2021**, 33, e2104681.

[118] Y. Gao, C. Xie, Z. Zheng, *Adv. Energy Mater.* **2020**, 11, 2002838.

[119] H. Sun, S. Xie, Y. Li, Y. Jiang, X. Sun, B. Wang, H. Peng, *Adv. Mater.* **2016**, 28, 8431-8438.

[120] Z. Wen, M. Yeh, H. Guo, J. Wang, Y. Zi, W. Xu, J. Deng, L. Zhu, X. Wang, C. Hu, *Sci. Adv.* **2016**, 2, e1600097.

[121] Z. Gao, P. Liu, X. Fu, L. Xu, Y. Zuo, B. Zhang, X. Sun, H. Peng, *J Mater. Chem. A* **2019**, 7, 14447-14454.

[122] G. Loke, T. Khudiyev, B. Wang, S. Fu, S. Payra, Y. Shaoul, J. Fung, I. Chatziveroglou, P. Chou, I. Chinn, W. Yan, A. Gitelson-Kahn, J. Joannopoulos, Y. Fink, *Nat. Commun.* **2021**, 12, 3317.

[123] O. Ozioko, R. Dahiya, *Adv. Intell. Syst.* **2021**, 4, 2100091.

[124] Y. Luo, Y. Li, P. Sharma, W. Shou, K. Wu, M. Foshey, B. Li, T. Palacios, A. Torralba, W. Matusik, *Nat. Electron.* **2021**, 4, 193-201.

[125] S. Hwang, M. Kang, A. Lee, S. Bae, S. Lee, S. Lee, T. Lee, G. Wang, T. Kim, *Nat. Commun.* **2022**, 13, 3173.

[126] J. Shao, X. Chen, X. Li, H. Tian, C. Wang, B. Lu, *Sci. China Technol. Sci.* **2019**, 62, 175-198.

[127] X. Hu, H. Wang, C. Zhai, H. Ge, Y. Cui, *J Mater. Chem. C* **2016**, 4, 11104-11109.

[128] M. Cenci, T. Scarazzato, D. Munchen, P. Dartora, H. Veit, A. Bernardes, P. Dias, *Adv. Mater. Technol.* **2021**, 7, 2001263.

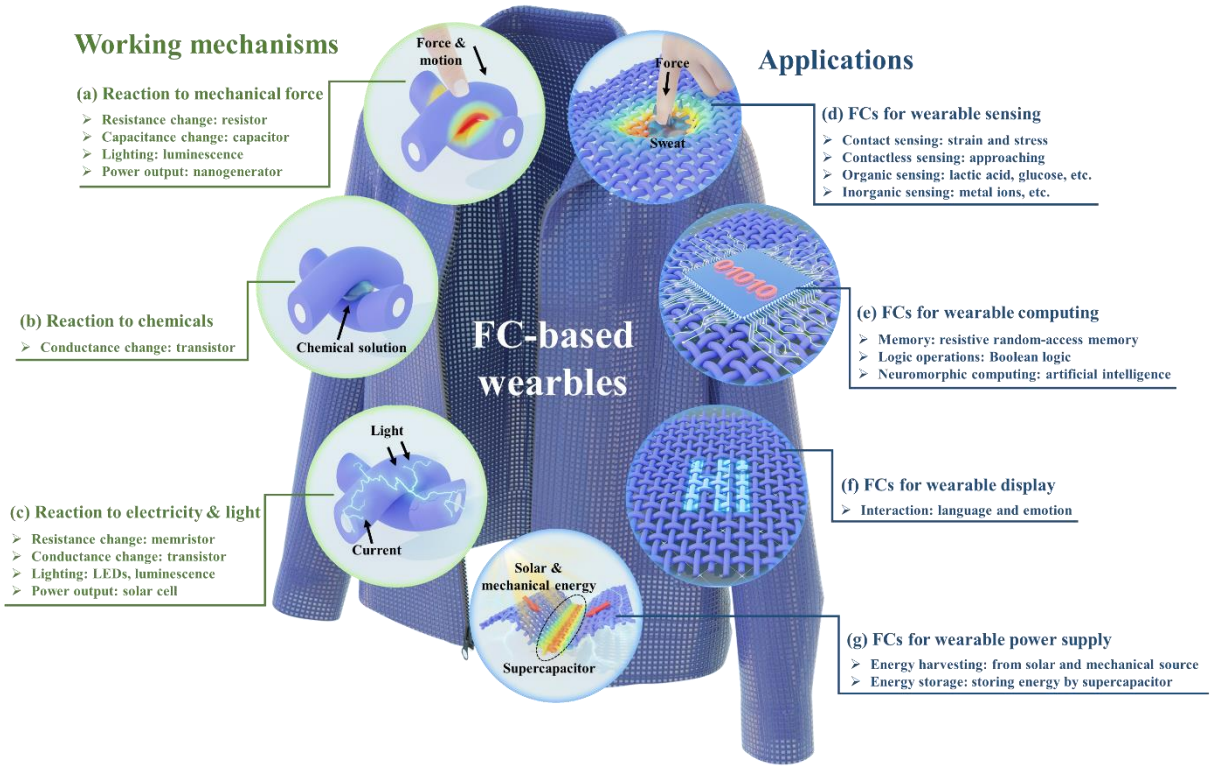

Figure 1. Overview of the FC-based systems. (a-c) Working mechanism of FCs: the resistance change, capacitance change, conductance change, lighting, and power output of FCs can be induced by various external stimuli, including (a) mechanical force, (b) chemicals, (c) and electricity and light signals. (d-g) Applications of FCs: (d) sensing, including contact and contactless methods, as well as organic and inorganic sensing; (e) computing, including data memory, logic operation, and neuromorphic computing; (f) display, including language and emotion interaction; and (g) power supply, including energy harvesting from solar and mechanical sources, as well as energy storage using supercapacitors.

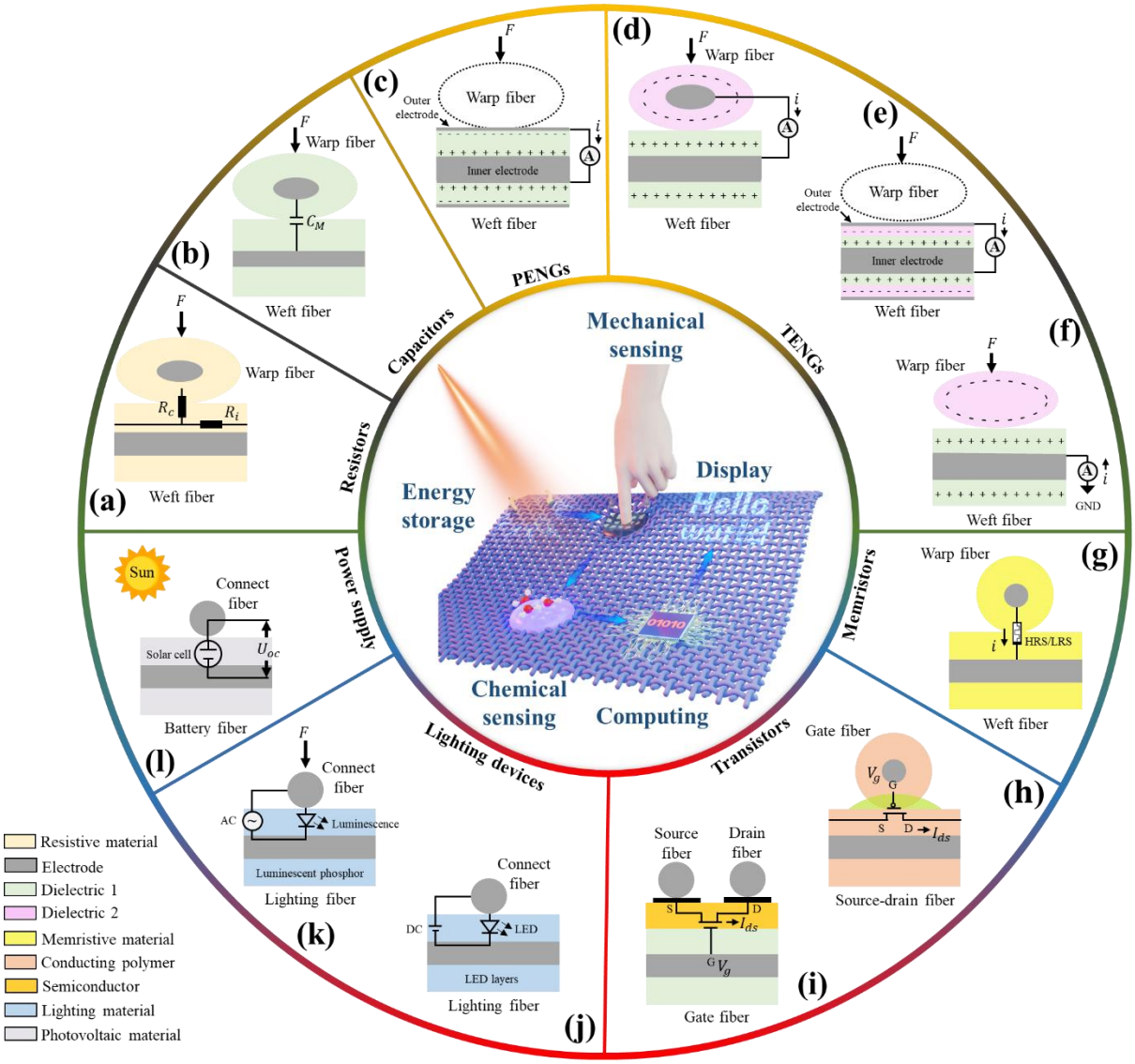

Figure 2. Design principles of FC-based devices. (a) FC-based resistor where the contact resistance (R_c) and internal resistance (R_i) change with applied pressure (F). (b) FC-based capacitor where the mutual capacitance (C_M) changes with F. (c) FC-based piezoelectric nanogenerator (PENG) where the piezoelectric potential and current are created and changed by F. (d-f) Three types of FC-based triboelectric nanogenerators (TENG), including two electrodes placed in (d) two fibers, (e) a single fiber, or (f) one fiber and ground, where the triboelectric potential and current are created and changed by F. (g) FC-based memristor where resistive switching between high resistance state (HRS) and low resistance state (LRS) happens when a programmable pulse is applied. (h-i) Two types of FC-based transistors: (h) FC-based organic electrochemical transistor (OECT) where the drain-source current (I_{ds}) changes with

the gate voltage (V_g) or when certain substances are added to the electrolyte; (i) FC-based field-effect transistor (FET) where I_{ds} changes with V_g. (j-k) Two types of FC-based lighting devices: (j) FC-based light-emitting diode (LED) where photons are released by applied DC voltage; (k) FC-based luminescence device where the luminescent phosphor of the lighting fiber releases photons by the applied AC voltage (electroluminescence) or by F (mechanoluminescence). (l) FC-based solar cell that generates an open-circuit potential (U_{oc}) under sunlight. Note: In this figure, weft fibers are shown as side sections, while warp fibers are shown as cross-sections.

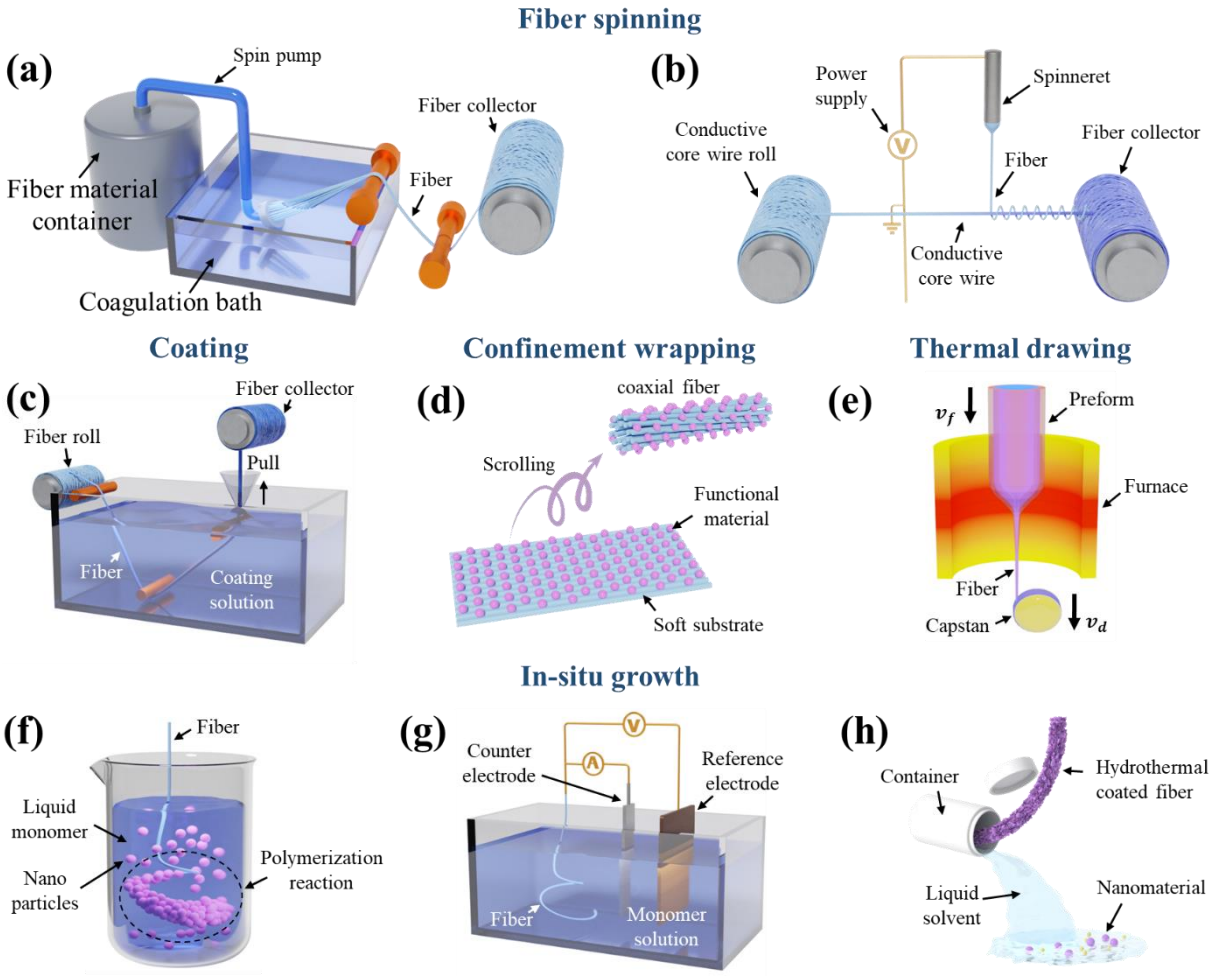

Figure 3. Common fabrication strategies of FC fibers. (a-b) Fiber spinning: (a) wet spinning; (b) electrospinning. (c) Coating. (d) Confinement wrapping. (e) Thermal drawing. (f-h) In-situ growth: (f) in-situ polymerization; (g) electroplating; (h) hydro/solvothermal processing.

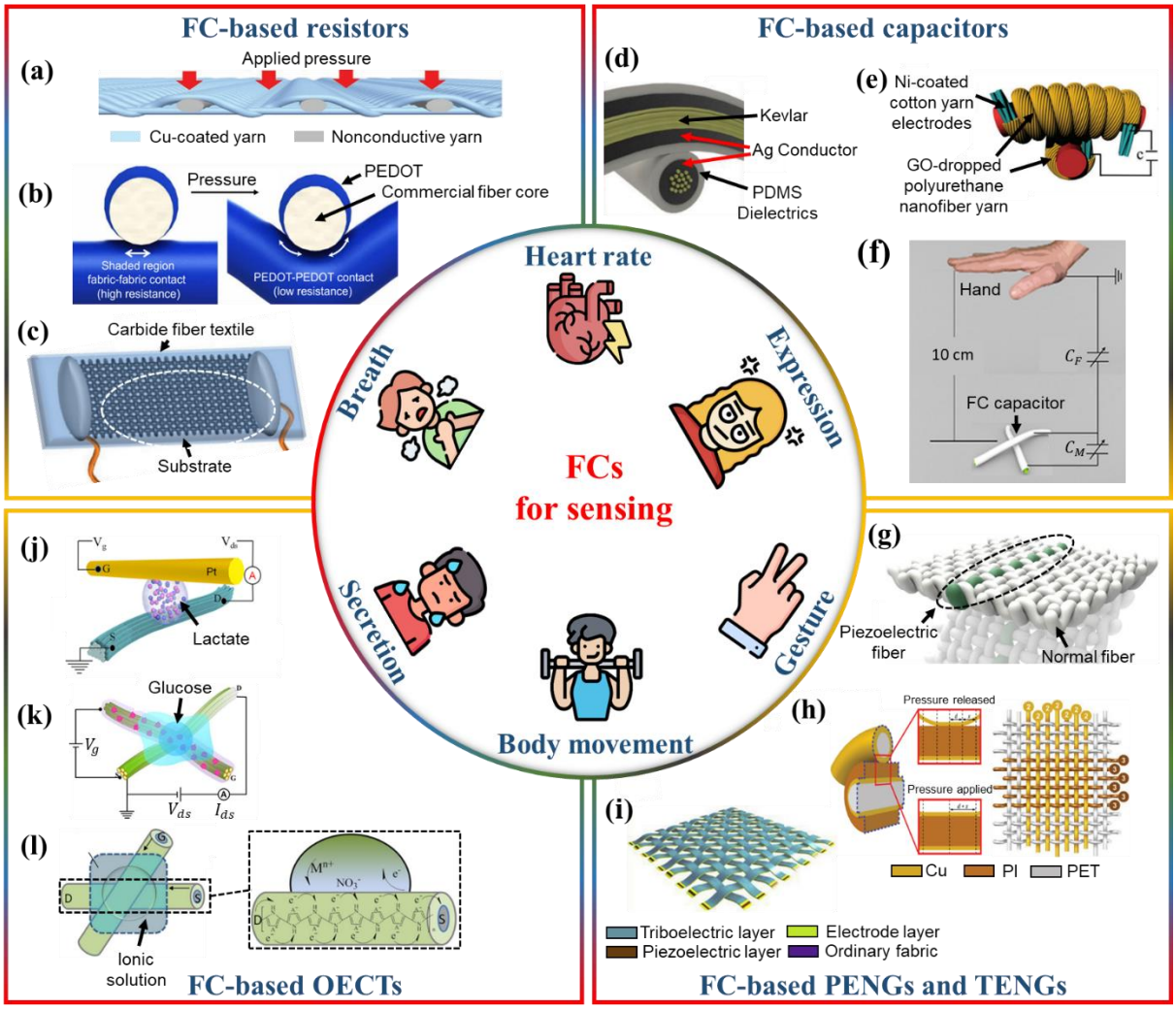

Figure 4. FCs for sensing. (a-c) FC-based resistors for mechanical sensing. (a) Schematic diagram of FC-based contact resistor sensor using Cu nanoparticles as resistive layers.[97] Reproduced with permission. Copywrite 2021, Wiley-VCH. (b) Schematic diagram of FC-based contact resistor sensor using PEDOT as resistive layers.[9] Reproduced with permission. Copywrite 2021, Science Publishing Group. (c) Schematic diagram of FC-based internal resistor sensor using carbonized silk as crack-generating material.[102] Reproduced with permission. Copywrite 2016, Wiley-VCH. (d-f) FC-based capacitors for mechanical sensing. (d) Schematic diagram of FC-based capacitor sensor using SBS-Ag nanoparticles as electrodes

and PDMS as dielectrics.[103] Reproduced with permission. Copywrite 2015, Wiley-VCH. (e) Schematic diagram of FC-based capacitor sensor using electro-spun GO-dropped polyurethane nanofiber yarns as dielectric layers.[40] Reproduced with permission. Copywrite 2018, The Royal Society of Chemistry. (f) Schematic diagram of FC-based capacitor sensor using Ag-bacterial cellulose and PDMS as electrodes and dielectric layers.[10] Reproduced with permission. Copywrite 2020, American Chemical Society. (g-i) FC-based PENGs and TENGs for mechanical sensing. (g) Schematic diagram of FC-based PENGs using PVDF and P(VDF-TrFE) as piezoelectric materials. Reproduced with permission. Copywrite 2020, MDPI.[104] (h) Schematic diagram of FC-based TENG sensor woven by Cu-PET fibers and PI-Cu-PET fibers.[14] Reproduced with permission. Copywrite 2016, Wiley-VCH. (i) Schematic diagram of PENG-TENG sensor.[46] Reproduced with permission. Copywrite 2019, Elsevier. (j-l) FC-based OECTs for chemical sensing. (j) Schematic diagram of FC-based OECT lactate sensor using MWCNT-doped PPy as channel layers.[67] Reproduced with permission. Copywrite 2020, Springer. (k) Schematic diagram of FC-based OECT glucose sensor using reduced GO-doped Ppy as channel layers.[105] Reproduced with permission. Copywrite 2017, Elsevier. (l) Schematic diagram of the FC-based OECT lead ion sensor using PPy and PVA-co-PE nanofibers as channel layers.[106] Reproduced with permission. Copywrite 2016, Springer.

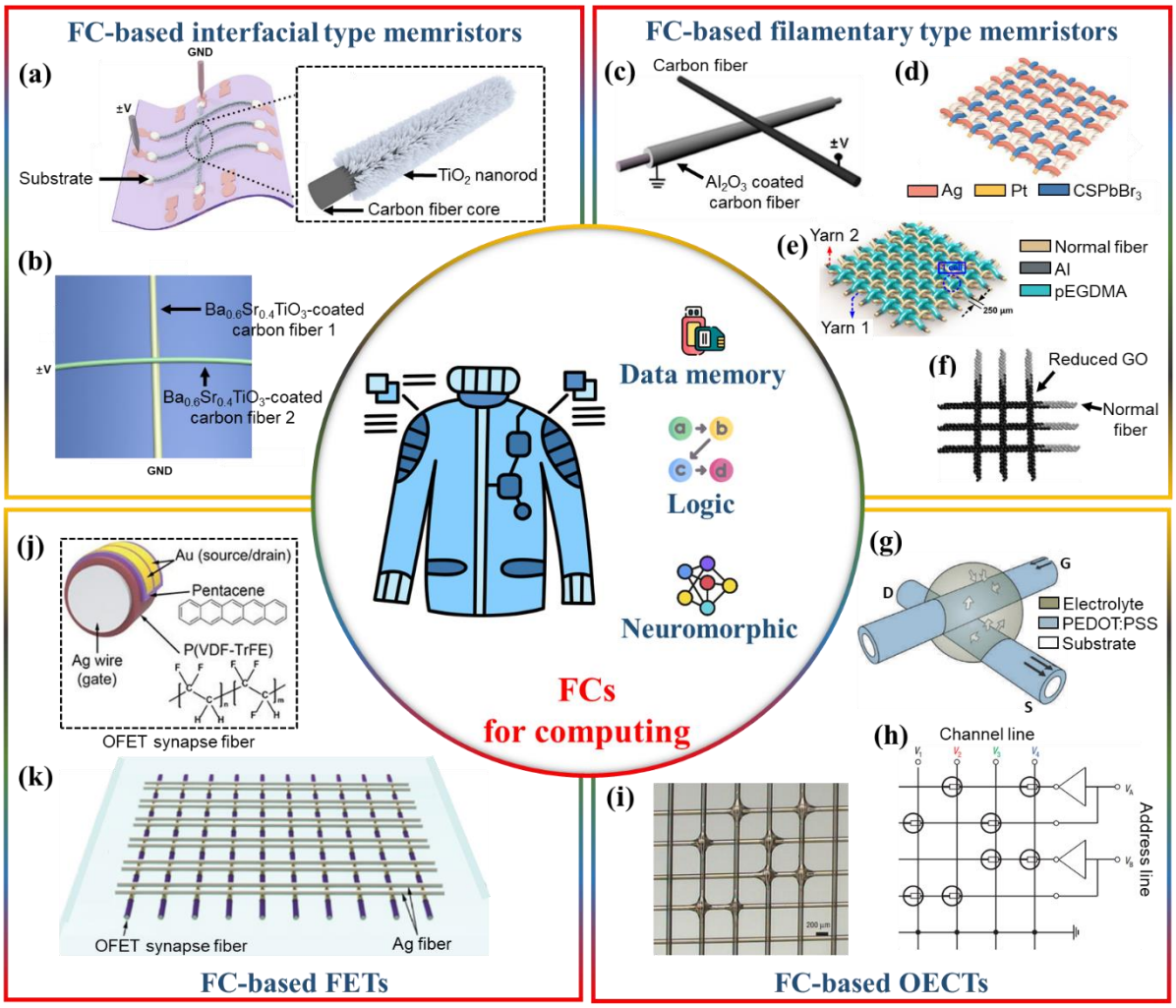

Figure 5. FCs for computing. (a-b) FC-based interfacial type memristors for computing. (a) Schematic diagram of FC-based interfacial type memristor RRAM using rutile TiO_2 nanorods coated on carbon fibers as memristive layers.[21] Reproduced with permission. Copywrite 2020, Elsevier. (b) Schematic diagram of FC-based interfacial type memristor synapse using $Ba_{0.6}Sr_{0.4}TiO_3$-coated carbon fibers as memristive layers.[60] Reproduced with permission. Copywrite 2020, Elsevier. (c-f) FC-based filamentary type memristors for computing. (c) Schematic diagram of FC-based electrochemical-metallization-filamentary type memristor RRAM using native Al_2O_3 layer as memristive layers.[20] Copywrite 2017, Wiley-VCH. (d) Schematic diagram of FC-based electrochemical-metallization-type filamentary memristor synapse using $CsPbBr_3$ as memristive layers.[110] Reproduced with permission. Copywrite 2022, Wiley-VCH. (e) Schematic diagram of FC-based TCM-type filamentary memristor RRAM

using pEGDMA as soft breakdown middle layers.[111] Reproduced with permission. Copywrite 2017, American Chemical Society. (f) Schematic diagram of FC-based electrochemical-metallization-type filamentary memristor synapse using $CsPbBr_3$ as memristive layers.[64] Reproduced with permission. Copywrite 2022, Wiley-VCH. (g-i) FC-based OECTs for computing. (g) Schematic diagram and (h) circuit photo of p-type FC-based OECT logic computing array.[19] Reproduced with permission. Copywrite 2007, Nature Publishing Group. (i) Schematic diagram of FC-based OECT using PEDOT:PSS and CNT as channels and electrodes.[27] Reproduced with permission. Copywrite 2021, Nature Publishing Group. (j) Schematic diagram of ferroelectric FC-based ferroelectric OFET synapse and (k) its array. Reproduced with permission.[114] Copywrite 2020, American Association for the Advancement of Science.

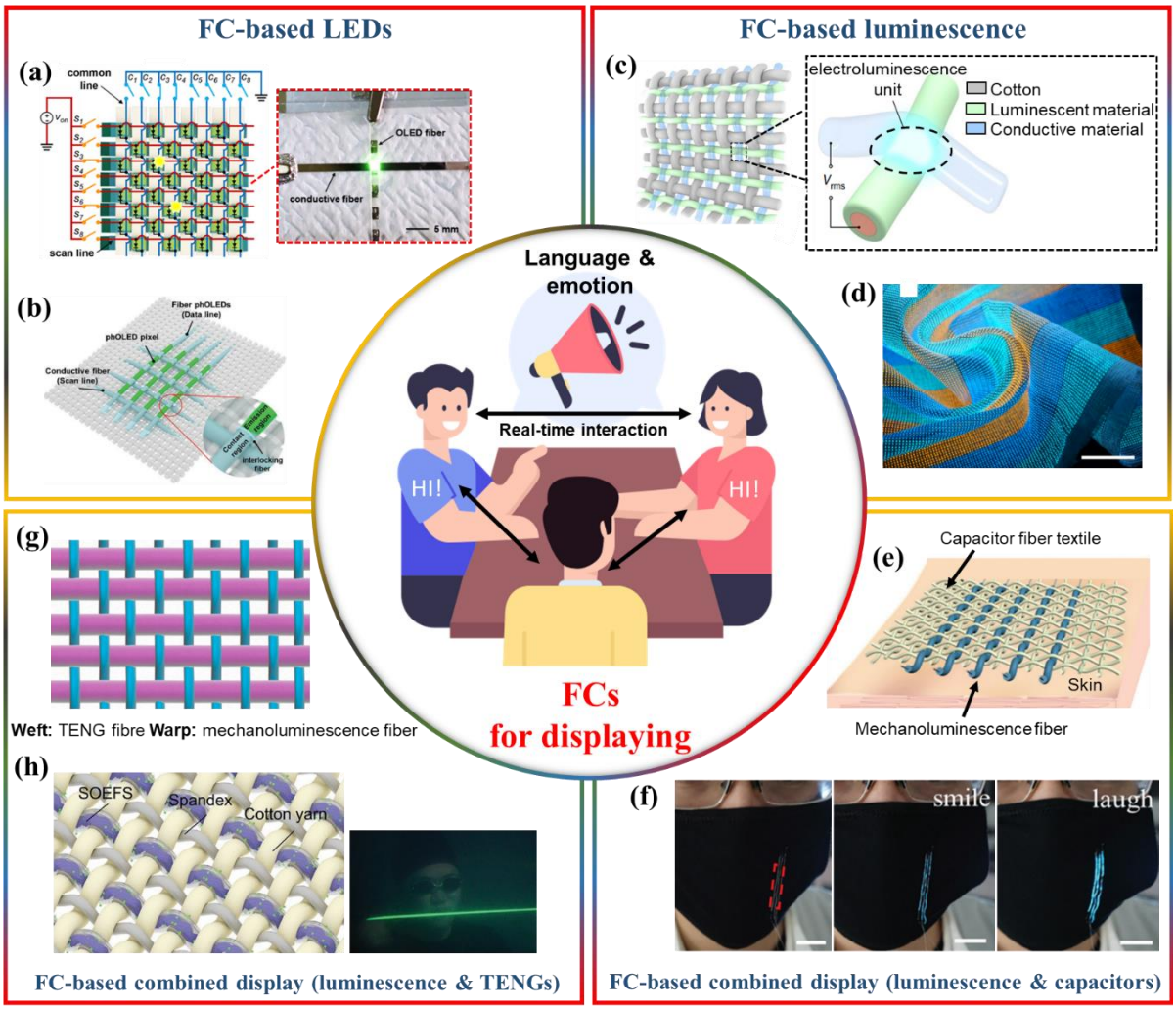

Figure 6. FCs for display. (a-b) FC-based LEDs for display. (a) Schematic diagram and photo of addressable FC-based LED array display.[75] Reproduced with permission. Copywrite 2019, American Chemical Society. (b) Schematic diagram of the OLED array display.[76] Reproduced with permission. Copywrite 2021, Wiley-VCH. (c-d) FC-based electroluminescence for display. (c) Schematic diagram and (d) photos of display textile containing 5×10^5 FC-based electroluminescence units.[12] Reproduced with permission. Copywrite 2021, Nature Publishing Group. (e-h) FC-based multifunctional displays. (e) Schematic diagram and (f) photos of FC-based mechanoluminescence-capacitors combined sensor.[79] Reproduced with permission. Copywrite 2020, The Royal Society of Chemistry. (g) Schematic diagram of wearable mechanoluminescence-TENGs fabric.[116] Reproduced with permission. Copywrite 2021, Elsevier. (h) Application of mechanoluminescence-TENGs for underwater work.[117]

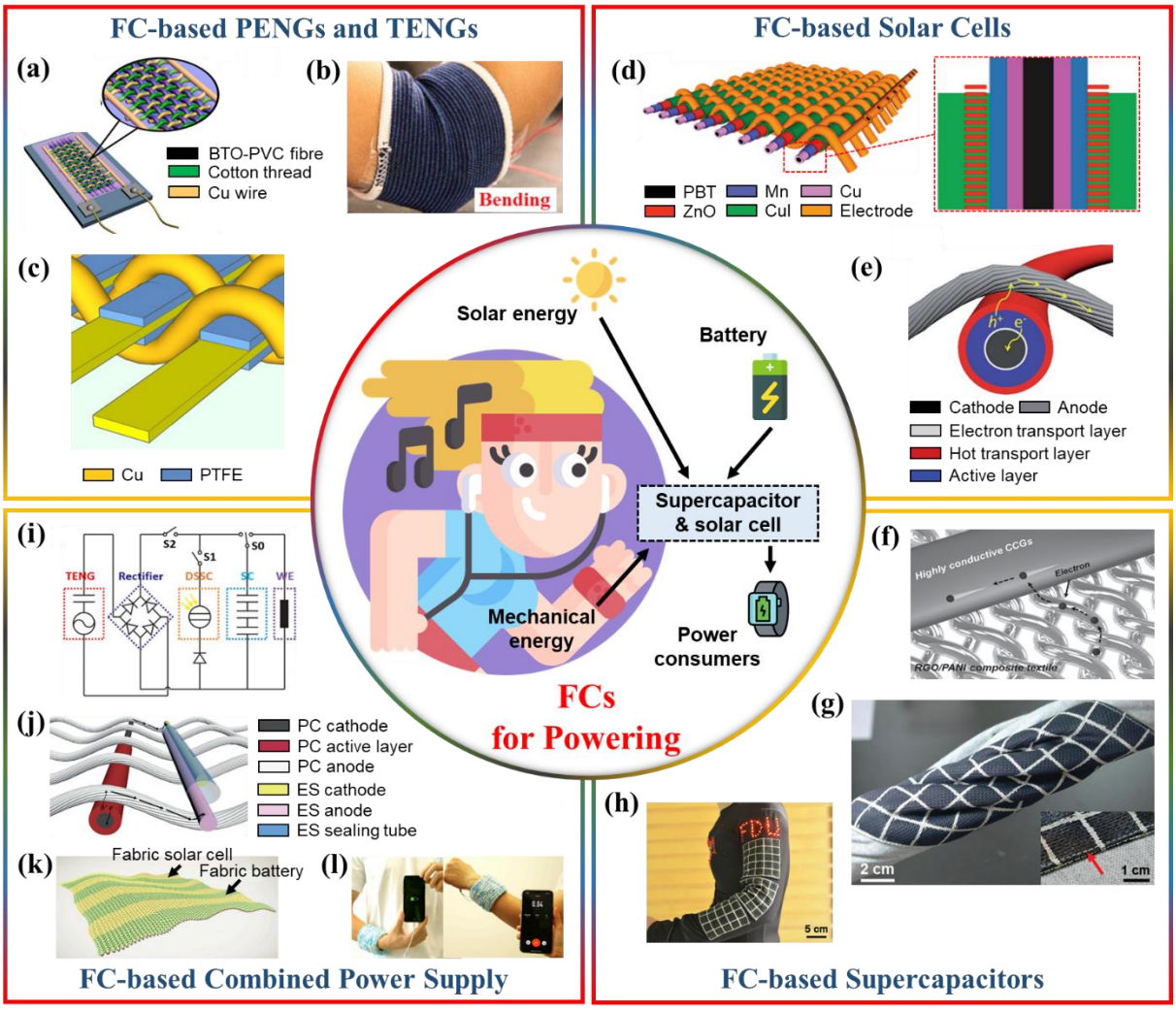

Figure 7. FCs for power supply. (a-c) FC-based PENGs and TENGs for energy harvesting. (a) Schematic diagram of FC-based PENG power supply using barium titanate nanowires as piezoelectric layers and (b) its bending test with elbows.[47] Reproduced with permission. Copywrite 2015, Elsevier. (c) FC-based TENGs using PTFE as triboelectric layers.[82] Reproduced with permission. Copywrite 2016, Nature Publishing Group. (d-e) FC-based solar cells for energy harvesting. (d) FC-based solar cell using ZnO-Mn, CuI, and Cu as photoanode, hole-transfer, and counter electrode material.[81] Reproduced with permission. Copywrite 2016, Wiley-VCH. (e) FC-based solar cell using PTB7:PC71BM and PEDOT:PSS as active and hole-transfer material.[83] Reproduced with permission. Copywrite 2018, The Royal Society of Chemistry. (f-h) FC-based supercapacitors for energy storage. (f) Schematic diagram and (g-h) photos of hierarchical FC-based supercapacitor.[119] Reproduced with permission. Copywrite

2016, Wiley-VCH. (i-k) FC-based multimodal power supply. (i) Circuit layout of highly integrated FC-based energy system.[120] Reproduced with permission. Copywrite 2016, Nature Publishing Group. (j) FC-based multimodal power supply comprised of solar cells and supercapacitors.[121] Reproduced with permission. Copywrite 2019, The Royal Society of Chemistry. (k) FC-based multimodal batteries that can be photovoltaic and chemical charged and (l) photos of it powering a cell phone.[79] Reproduced with permission. Copywrite 2020, Cell Press.

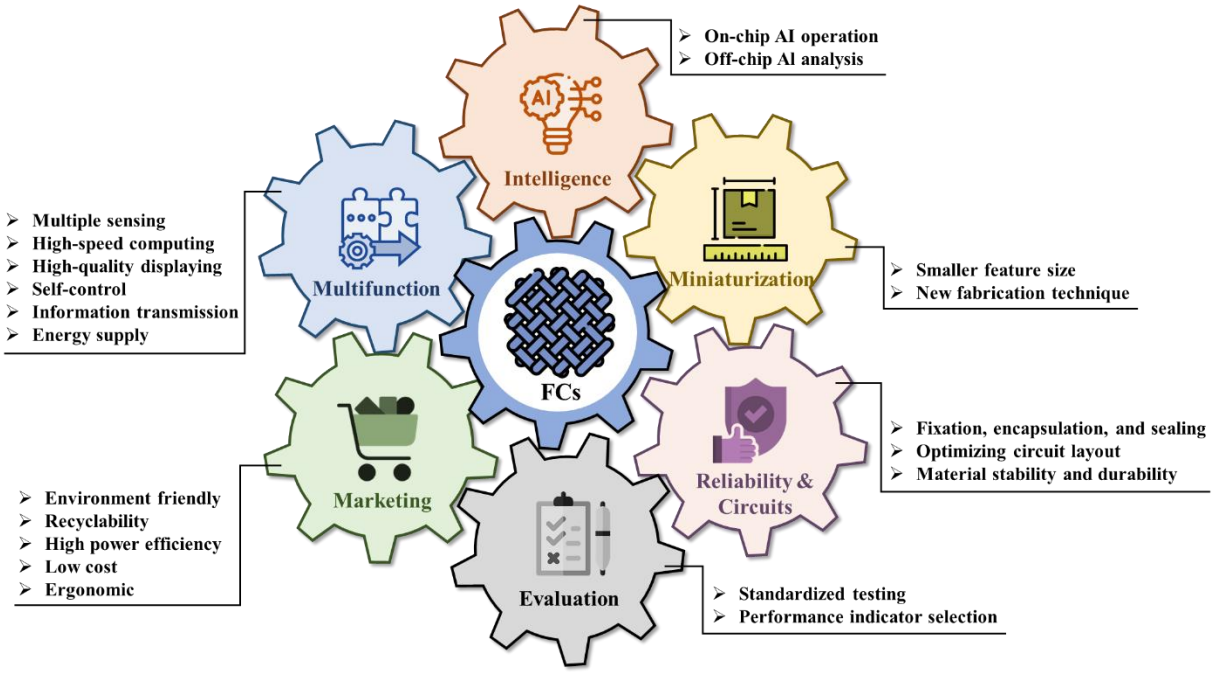

Figure 8. Trends and challenges of FC-based systems.

Figure 9. FC-based systems for the future.